



The University of Bradford Institutional Repository

<http://bradscholars.brad.ac.uk>

This work is made available online in accordance with publisher policies. Please refer to the repository record for this item and our Policy Document available from the repository home page for further information.

To see the final version of this work please visit the publisher's website. Available access to the published online version may require a subscription.

Link to publisher's version: <https://doi.org/10.1680/jgein.17.00033>

Citation: Mirzababaei M, Mohamed MHA, Arulrajah A, Horpibulsuk S and Anggraini V (2018) Practical approach to predict the shear strength of fibre-reinforced clay. *Geosynthetics International*. 25(1): 50–66.

Copyright statement: © 2018 ICE. Reproduced in accordance with the publisher's self-archiving policy.

Practical approach to predict the shear strength of fibre-reinforced clay

Mehdi Mirzababaei, B.Eng., MSc., PhD (Corresponding author)

Lecturer, School of Engineering and Technology

Central Queensland University, 120 Spencer Street, Melbourne, Victoria 3000, Australia

Email: m.mirzababaei@cqu.edu.au

Tel: +61 3 9610626

Mostafa Mohamed, B.Eng., MSc., PhD

Senior Lecturer, University of Bradford, Faculty of Engineering and Informatics, Bradford, BD7 1DP, the UK

Email: m.h.a.mohamed@bradford.ac.uk

Arul Arulrajah, BSc, MEngSc, PhD

Professor, Department of Civil and Construction Engineering

Swinburne University of Technology, Hawthorn, Victoria 3122, Australia

Email: arulrajah@swin.edu.au

Suksun Horpibulsuk, Professor and Chair, School of Civil Engineering,

Director, Centre for Innovation in Sustainable Infrastructure Development,

Suranaree University of Technology, Nakhon Ratchasima 30000, Thailand

Email: suksun@g.sut.ac.th

Vivi Anggraini, B.Eng., M.Eng. Ph.D

Lecturer, School of Engineering, Monash University Malaysia

Jalan Lagoon Selatan, 47500 Bandar Sunway, Selangor Darul Ehsan, Malaysia

Email: vivi.anggraini@monash.edu

Total number of words (main text excluding abstract and refs): 5643

Number of Figures: 19

Number of Tables: 3

Abstract

1 Carpet waste fibres have a higher volume to weight ratios and once discarded into landfills, these fibres occupy a
 2 larger volume than other materials of similar weight. This research evaluates the efficiency of two types of carpet
 3 waste fibre as sustainable soil reinforcing materials to improve the shear strength of clay. A series of consolidated
 4 undrained (CU) triaxial compression tests were carried out to study the shear strength of reinforced clays with 1%,
 5 to 5% carpet waste fibres. The results indicated that carpet waste fibres improve the effective shear stress ratio and
 6 deviator stress of the host soil significantly. Addition of 1%, 3% and 5% carpet fibres could improve the effective
 7 stress ratio of the unreinforced soil by 17.6%, 53.5% and 70.6%, respectively at an initial effective consolidation
 8 stress of 200 kPa. In this study, a nonlinear regression model was developed based on a modified form of the
 9 hyperbolic model to predict the relationship between effective shear stress ratio, deviator stress and axial strain of
 10 fibre-reinforced soil samples with various fibre contents when subjected to various initial effective consolidation
 11 stresses. The proposed model was validated using the published experimental data, with predictions using this model
 12 found to be in excellent agreement.

13

14 **Key words:** Geosynthetics, Shear strength, Carpet waste fibre, Reinforced soil, Clays, Modified hyperbolic model

Notations:

Basic SI units are shown in parentheses.

15	q_{ratio}	deviator stress ratio (dimensionless)
16	p'_{ratio}	average mean effective stress ratio (dimensionless)
17	q	deviator stress (Pa)
18	p'	mean effective stress (Pa)
19	q_{re}	deviator stress of fibre-reinforced soil (Pa)
20	q_{un}	deviator stress of unreinforced soil (Pa)
21	$(\frac{q}{p'})_{re}$	effective stress ratio of fibre-reinforced soil (dimensionless)
22	$(\frac{q}{p'})_{un}$	effective stress ratio of unreinforced soil (dimensionless)
23	p'_{re}	mean effective stress of fibre-reinforced soil (Pa)
24	p'_{un}	mean effective stress of unreinforced soil (Pa)
25	σ'_1	major principal effective stress (Pa)
26	σ'_3	minor principal effective stress (Pa)
27	z, w	coefficients of the linear relationship between q_{ratio} and p'_{ratio} (dimensionless)
28	ε	axial strain in triaxial shear test (dimensionless)
29	a, b, n, g, h, t	modified hyperbolic model parameters (dimensionless)
30	$a^*, b^*, n^*, g^*, h^*, t^*$	normalised modified hyperbolic model parameters (dimensionless)
31	σ'_c	initial effective consolidation stress (Pa)
32	f	fibre content (dimensionless)
33	$k_{1a,g}, k_{2a,g}, k_{1b,h}, k_{2b,h}, k_{1n,t}, k_{2n,t}$	coefficients of the linear equations for normalised model parameters
34	(dimensionless)	

1. Introduction

35 The carpet manufacturing industry produces a large quantity of fibre wastes due to aspects such as the end of line
36 leftovers, stop-start wastage, yarn breakages, faults and quality control. In addition, as the demand for new carpets
37 increases, substantial amounts of old and post-consumer carpet wastes have to be disposed to landfills. Synthetic
38 fibres used in carpet manufacturing are particularly problematic as they do not degrade with time and once dumped
39 into landfills, may release colour pigments in the surrounding soil. This may pollute the underground water
40 reservoirs, which are potential sources for domestic use. Local communities, businesses and governmental agencies
41 are increasingly encouraged to re-use and recycle carpet waste fibres, so as to minimise the need for landfilling.
42 Virgin discrete synthetic/natural fibres have been used in geotechnical engineering practice to improve the stress-
43 strain response of fine and coarse-grained soils. Upon mixing with soil particles, short discrete fibres behave like
44 tension resisting elements interlocking soil particles to partially withstand shear stresses within the soil. This results
45 in the formation of a composite coherent soil matrix that possesses superior strength properties with reduced and/or
46 eliminated continuous planes of weakness at failure (Ahmad et al., 2010). The reinforcing role of short virgin
47 synthetic fibres in coarse-grained soils with loose to dense states has been studied previously (Maher and Gray 1990;
48 Nataraj 1997; Consoli et al. 2007; Diambra et al. 2007, 2010; Chen and Loehr 2009; Hamidi and Hooresfand 2013;
49 Miranda Pino et al. 2015; and Jamsawang et al. 2015). The behaviour of fibre-reinforced fine-grained soils has also
50 been studied previously (Falorca et al. 2006; Casagrande et al. 2006; Özkul and Baykal 2007; Al-Akhras et al. 2010;
51 Babu and Chouksey 2010; Ekinici and Ferreira 2012; Maliakal and Thiyyakkandi 2013; Sadeghi and Beigi 2014 and
52 Botero et al. 2015; Khatri et al. 2015; and Anggraini et al. 2016). The reported research findings are in agreement in
53 that fibre reinforcement improves the stress-strain behaviour, unconfined compression strength, shear strength and
54 ductility of the soil and reduces the consolidation settlement of clay. Currently, the research theme within the area of
55 soil fibre reinforcement is strongly favoured towards the use of virgin short fibres, mostly with granular soils. There
56 is presently a research gap on the utilisation of recycled carpet waste fibres for the reinforcement of clays, with only
57 limited current publications on this aspect (Murray et al. 2000, Ghiassian et al. 2004, Fatahi et al. 2012, 2013 a & b
58 and Mirzababaei et al. 2013 a & b, 2017 b).

59 Murray et al. (2000) conducted a consolidated undrained compression triaxial testing program to investigate the
60 shear strength of a reinforced sandy silt soil with nylon waste fibres and virgin fibrillated polypropylene fibres. The
61 results indicated that adding up to 3% waste nylon fibre or a maximum of 1% polypropylene virgin fibre can
62 significantly increase the peak shear strength of the soil and can reduce its post-peak reduction in a ductile manner.
63 Based on a series of drained compression triaxial tests on sand samples reinforced with carpet waste strips,
64 Ghiassian et al. (2004) reported a satisfactory degree of improvement in the peak shear strength of sand that could
65 be achieved by either increasing the strip content at a constant aspect ratio or by increasing the aspect ratio at a
66 constant strip content.

67 Recently, Fatahi et al. (2012, 2013 b) reported the improving effect of carpet waste fibre addition to cement
68 stabilised soft kaolin and stated that the fibre type and content could significantly influence the peak shear strength,

69 stiffness and brittleness of the soft clays. The initial Young's modulus of the cement-stabilised clay increased with
70 the addition of polypropylene fibres, but reduced with the addition of carpet and steel fibres.

71 Mirzababaei et al. (2013 a and b) carried out an extensive testing programme to investigate the unconfined
72 compression strength and swelling pressure of expansive clays reinforced with carpet waste fibres and concluded
73 that inclusion of up to 5% carpet waste fibres could result in reduction of the swelling pressure and increasing the
74 unconfined compression strength of the clay. However, the relative gain in unconfined compression strength and
75 reduction in swelling pressure is highly dependent on the initial dry unit weight and the moisture content of the clay.
76 Mirzababaei et al. (2017 b) also reported significant enhancement in the bearing capacity of a model footing on a
77 clay slope reinforced with carpet waste fibre. In this study, the stress-strain behaviour of a clay reinforced with two
78 types of carpet waste fibre was analysed by conducting a number of consolidated undrained triaxial compression
79 tests. Thus the experimental programme in this research seeks to evaluate the feasibility to sustainably reuse carpet
80 waste fibres with non-uniform lengths and thicknesses to enhance the shear strength of clay.

81 Several analytical models are available to estimate the stress-strain behaviour of fibre-reinforced granular soils
82 based on the force-equilibrium approach (Waldron 1977; Gray and Ohashi 1983; Maher and Gray 1990; Ranjan et
83 al. 1996; Michalowski 2008; Shukla et al. 2010), energy-based model (Michalowski and Zhao 1996) and discrete
84 framework model (Zornberg 2002). There are also several statistical models to predict the shear strength of fibre-
85 reinforced granular soils (Ranjan et al 1996; Babu and Vasudevan 2008) with input parameters including some or
86 any of the following: fibre content, fibre aspect ratio, fibre surface friction, confining pressure, fibre length, cohesion
87 and internal friction angle of the fibre-reinforced soil. Cam Clay constitutive model has also been reformulated to
88 account for the estimation of the deviator stress of fibre-reinforced clays (Chen 2007; Babu and Chouksey 2010;
89 Diambra and Ibraim 2014 and Nguyen and Fatahi 2016).

90 Although all proposed analytical and constitutive models agree well with the experimental data, the parameters
91 required to execute these models are complex and require a number of triaxial, direct shear and consolidation tests.
92 Therefore, due to the variability of soil types, fibre types and the complex interfacial behaviour of the soil at the
93 interface with fibres, it is required to estimate the shear strength properties of the fibre-reinforced soil with less
94 effort, so as to obtain the soil/fibre input parameters to ease its application in practice. In this study, a simple
95 regression model is developed to predict the relationship between the effective shear strength ratio (q/p'), deviator
96 stress (q) and the axial strain of a fibre-reinforced clay subjected to axial deviator stress at any fibre content and
97 confining pressure regardless the fibre type and clay type.

2. Materials

98 The soil sample used in this study was collected from a site in the Northwest region of the United Kingdom. The soil
99 was classified as low plastic clay according to the Unified Soil Classification System (USCS) with a plasticity index
100 of 17% and specific gravity of 2.68. The grain size analysis of the soil indicated that it contained 55.78% fine grains
101 and 44.22% coarse grains. **Table 1** shows the properties of the soil. Two different types of carpet waste fibre (i.e.,
102 herein called GBF and ABF) were utilised in this investigation and supplied by Carpet Recycling UK and Milliken
103 Carpet Europe as waste by-products from the production line (i.e. from shearing and/or edge trimming of the

104 carpet). The GBF consisted predominantly of propylene fibres whereas the ABF included short nylon fibres. **Table**
105 **2** presents typical specifications of the carpet waste fibres used in this study. Due to the waste origin of the fibres
106 used in this study, the length of the fibres ranged from 2 to 20 mm with diverse thicknesses from 80 μm to 1,500
107 μm .

3. Experimental Programme

108 In this study, because carpet fibre is classified as waste material, it was decided to investigate the addition of a high
109 proportion of waste fibres on the shear strength of the clay. Therefore, fibre contents of 1%, 3%, and 5% of the dry
110 mass of soil were selected to reinforce the clay. Because of reduced workability and practical difficulties to mix
111 higher fibre contents evenly with the soil, the maximum fibre content used in this study was limited to 5%. Standard
112 Proctor compaction tests were carried out on the unreinforced and fibre-reinforced clay. The compaction test results
113 revealed that the maximum dry unit weight of the soil decreases with fibre inclusion. **Figure 1** presents the
114 compaction curves of the unreinforced and carpet waste fibre-reinforced soil with both fibre types. To achieve a
115 uniform distribution of fibres in the clay sample, various approaches were undertaken including mixing water
116 soaked fibres with dry clay, addition of dry fibres to the wet clay followed by mixing and mixing dry clay and fibres
117 followed by spraying water on the mixture. It was concluded that spraying water on a dry mixture of fibre and clay
118 to achieve the desired moisture content results in producing relatively uniform samples with less fibre tangling.
119 However, other examined methods led to the formation of fibre lumps or balling during preparation that could affect
120 the homogeneity of the sample. Therefore, the dry soil and fibres were mixed thoroughly in a sealed container by
121 shaking. Subsequently, the calculated amount of water to reach the target moisture content was sprayed over the dry
122 mixture of soil and fibre in several stages, followed by hand mixing to prepare a uniform mixture. The prepared
123 mixture was kept in a sealed container for 3 to 4 days before the test day. This procedure, could possibly increase the
124 mixing efficiency and therefore, ensure a relative uniformity of fibre distribution in the fibre-reinforced soil sample.

125 A series of consolidated undrained triaxial tests were carried out on unreinforced and fibre-reinforced clay samples
126 following BS 1377-8:1990 standard. Unreinforced and fibre-reinforced cylindrical clay samples with a diameter of
127 38 mm and height of 76 mm were prepared at the same dry unit weight of 17.8 kN/m^3 and their equivalent moisture
128 content on the dry side of the compaction curve (refer to **Figure 1**; see solid points). Soil samples were saturated
129 with a B Skempton ratio of at least 0.97 using steps of back pressure and cell pressure and subsequently
130 consolidated at initial effective consolidation stresses of 50 kPa, 100 kPa and 200 kPa, respectively to simulate the
131 medium to relatively high in-situ effective stress ranges and consequently sheared at axial strain rate of 0.13%/min.
132 There are a few studies investigating the effect of sample size on the unconfined compression strength (UCS) and
133 shear strength of fibre-reinforced clays. Xiao et al., (2014) experienced a significant increase in the UCS of 7-day
134 cured fibre-reinforced clay when the sample size increased from 50 mm to 100 mm. However, the change was minor
135 when the sample size was changed from 100 mm to 150 mm. They also reported insignificant size effect on UCS of
136 14-day and 28-day cured fibre-reinforced samples. They also investigated the consolidated undrained and
137 consolidated drained shear strength of fibre-reinforced clay and found that up to the consolidation stress of 110 kPa,
138 the sample size does not affect the deviator stress of the fibre-reinforced clay significantly.

139 Nataraj and McManis (1997) also investigated the mechanical behaviour of fibre-reinforced clay using UCS test,
 140 direct shear test and CBR test. They reported an increase in UCS with the increase in sample size from 33 to 70 mm.
 141 However, they found the strength of 100 mm fibre-reinforced sample was slightly lower than that for 70 mm
 142 sample. Ang and Loehr (2003) also investigated the effect of sample size on the UCS of clays with diameter from 38
 143 mm to 152 mm. They observed the highest UCS for 70 mm samples. They also concluded that sample size
 144 influences the UCS of the clay compacted at dry side of the optimum value significantly. Therefore, although there
 145 are no definite published results confirming the effect of sample size on the shear strength of clays in consolidated
 146 triaxial tests, a sample diameter to fibre length ratio of 8 is desirable as recommended by Xiao et al. (2014). In this
 147 study, due to the waste origin of the carpet fibres and their random size including fibre lengths from 2 mm to 20 mm
 148 and fibre diameters from 80 μm to 1,500 μm , the above criteria may have been met partially as there was no control
 149 on picking appropriate fibre lengths for sample preparation. On the other hand, smaller samples may not allow full
 150 mobilisation of the reinforcing role of fibres in fibre-reinforced soil resulting in underestimating the shear strength
 151 of fibre-reinforced clay (Ang and Loehr 2003).

4. Results and Discussions

152 The contributing effect of fibre reinforcement on the shear strength behaviour of clay samples in terms of deviator
 153 stress ratio-mean effective stress ratio (q_{ratio}/p'_{ratio}), effective stress ratio (q/p') and deviator stress (q) versus
 154 axial strain was analysed and discussed in the following sections.

4.1. Effective stress ratio and deviator stress of fibre-reinforced clay

155 The stress-strain relationships during the consolidated undrained triaxial test were normalised and plotted for
 156 effective stress ratio (q/p') and deviator stress versus axial strain for both unreinforced and fibre-reinforced soil
 157 samples at different initial effective consolidation stresses of 50 kPa, 100 kPa and 200 kPa as shown in **Figures 2**
 158 **and 3**. **Figure 2** shows that inclusion of GBF fibre enhanced the effective stress ratio and deviator stress of the host
 159 soil significantly. Based on the graphs shown in **Figure 2a**, fibre-reinforced soil with 1%, 3% and 5% GBF fibre
 160 content improved the effective stress ratio of the unreinforced soil at initial effective consolidation stress of 200 kPa
 161 by 17.6%, 53.5% and 70.6%, respectively (i.e., measured at an axial strain of 20%). Although the effective stress
 162 ratios of the fibre-reinforced soil with 3% and 5% GBF fibre contents were almost similar at all effective
 163 consolidation stresses, their deviator stress behaviour was markedly different. This is mainly due to a simultaneous
 164 increase in both deviator stress and mean effective stress with the increase in fibre content resulting in less growth in
 165 effective stress ratio with the increase in fibre content. The ratio of deviator stress of 5% fibre-reinforced soil to that
 166 of 3% fibre-reinforced soil at an axial strain of 20% measured for initial effective consolidation stress of 200 kPa
 167 was determined to be 2.43 for GBF fibre-reinforced soil. The inclusion of 1%, 3% and 5% GBF fibre improved the
 168 deviator stress of the soil by 4.0%, 35.3% and 229.4% for the test with initial effective consolidation stress of 200
 169 kPa (i.e., measured at an axial strain of 20%).

170 ABF fibre-reinforced soils also demonstrated significant improvement in effective stress ratio and deviator stress
 171 over those of unreinforced soil. At an axial strain of 20%, ABF fibre-reinforced soil samples subjected to initial
 172 effective consolidation stress of 200 kPa, produced 20.0%, 32.4% and 37.5% effective stress ratio improvement with

173 inclusion of 1%, 3% and 5% fibre, respectively (see **Figure 3a**). The inclusion of 1%, 3% and 5% ABF fibre, also
 174 improved the deviator stress of the soil by 16.7%, 38.4% and 129.3% at initial effective consolidation stress of 200
 175 kPa (i.e., measured at an axial strain of 20%, **Figure 3b**). Fibre-reinforced soil samples with 3% fibre showed
 176 slightly higher effective stress ratio at initial effective consolidation stress of 50 kPa than that of 5% fibre-reinforced
 177 soil samples (See **Figures 2a and 3a**). However, with an increase in initial effective consolidation stress to 100 kPa
 178 and 200 kPa, the observed order was reversed. This observation for the behaviour of fibre-reinforced soil is
 179 consistent with results previously reported by Freilich and Zornberg (2010) as they observed an increase in
 180 effectiveness of fibres on the shear strength of the soil with the increase in the effective confining pressure. At
 181 higher initial effective consolidation stresses prior to the shearing stage, due to increase in confining pressure and
 182 hence improved interaction between soil particles and fibres, the fibres were increasingly stretched. Therefore, upon
 183 initiating the shear stage, the fibres contribute better to distributing the applied shear stresses into a wider area.
 184 However, at lower initial effective consolidation stresses, the fibres may not interact effectively with soil grains and
 185 hence may slip in shear. Hence at relatively low confining stresses, the fibres may not effectively confine soil grains
 186 nor add surplus strength to the reinforced soil. Therefore, an increase in the fibre content at a low initial effective
 187 consolidation stress may have an adverse effect on the strength of the reinforced soil without necessary soil grain
 188 harnessing effect.

189 **Figures 2 and 3** also demonstrate that inclusion of fibres resulted in turning the plastic stress-strain behaviour of the
 190 unreinforced soil to a strain hardening behaviour. The shear strength behaviour of a soil is partly dependent on its
 191 initial moisture content and dry unit weight (Lamb and Whitman 1979). Reduction in the dry unit weight and
 192 increase in the moisture content of a soil mass subjected to shear stresses results in a rapid shear failure (Newcomb
 193 and Birgisson 1999). Although the moisture contents of the prepared soil samples were different and increased with
 194 fibre content, the shear strength ratio of the fibre-reinforced soil was superior to that of the unreinforced soil. The
 195 observed stress-strain response indicated that the contribution of the fibres to improve the shear strength of the soil
 196 samples prepared at an identical dry unit weight and different moisture contents, compensated for the loss of shear
 197 strength due to an increase in moisture content of the fibre-reinforced soil samples.

198 Repeatability and reliability of the shear strength test results of the fibre-reinforced soil are paramount for acquiring
 199 an accurate mechanical behaviour, deeper understanding and successful modelling of the fibre-reinforced clay
 200 behaviour. Although, a consistent and careful control was undertaken during the sample preparation phase to ensure
 201 uniform distribution of fibres within the clay sample, to confirm the reliability of results three tests repeated on the
 202 fibre-reinforced clay samples with 5% ABF fibre content at initial consolidation stresses of 50, 100 and 200 kPa,
 203 respectively. **Figure 4** compares the original and the repeat test results and shows a good repeatability of the results.
 204 In this study, the deviator stress ratio and mean effective stress ratio are defined as the ratio of the deviator and mean
 205 effective stress of the fibre-reinforced soil to that of the unreinforced soil, respectively:

$$206 \text{ Deviator stress ratio } (q_{ratio}) = \frac{q_{re}}{q_{un}} \quad (\text{Eq.1})$$

$$207 \text{ Mean effective stress ratio } (p'_{ratio}) = \frac{p'_{re}}{p'_{un}} \quad (\text{Eq.2})$$

208 where; q is the deviator stress ($\sigma'_1 - \sigma'_3$), p' is the mean effective stress ($(1/3)(\sigma'_1 + 2\sigma'_3)$) and $\sigma'_{1,3}$ are the major and

209 minor principal effective stresses

210 Note: re: reinforced, un: unreinforced

211 **Figure 5** presents the relationships between q_{ratio} and p'_{ratio} of the fibre-reinforced soil samples. Illustrated data in
 212 this figure are related to the data of q_{ratio} , and p'_{ratio} of the fibre-reinforced soil samples subjected to initial
 213 effective consolidation stresses of 50 kPa, 100 kPa and 200 kPa and calculated at axial strains of 5%, 10%, 15% and
 214 20%, respectively. **Figure 5** also shows that q_{ratio} changed rather linearly with p'_{ratio} at all fibre contents for both
 215 fibre types and the deviator stress ratio and mean effective stress ratio of the fibre-reinforced soil increased with
 216 fibre content. Assuming q_{ratio} a linear function of p'_{ratio} , we can write:

$$217 \quad q_{ratio} = z \times p'_{ratio} + w \quad (Eq.3)$$

218 **Equation 3** shows that a linear relationship existed between the deviator stress ratio and mean effective stress ratio
 219 of the fibre-reinforced soil. However, this equation did not specifically elaborate on the above relationship as a
 220 function of axial strain during triaxial compression test, fibre content and initial consolidation stress of the soil
 221 sample. Therefore, it is required to develop models to correlate the effective stress ratio and deviator stress of the
 222 fibre-reinforced soil to the axial strain, fibre content and initial consolidation stress of the clay sample during the
 223 triaxial compression test.

4.2. Predicting the effective stress ratio and deviator stress of fibre-reinforced soil

224 Duncan-Chang model (i.e., hyperbolic stress-strain theory, 1970) is an incremental nonlinear stress-dependent
 225 model that explains the nonlinearity, stress-dependent and inelastic behavioural feature of cohesive and cohesionless
 226 soils with a simple form. Horpibulsuk and Miura (2001) and Horpibulsuk and Rachan (2004) used a modified form
 227 of the Duncan-Chang hyperbolic model to capture the undrained and drained behaviour of uncemented and cement
 228 stabilised clays. The modified hyperbolic model can exhibit strain softening behaviour following the destruction of
 229 the sample at peak and also the strain hardening behaviour. Therefore, in this study, the modified hyperbolic model
 230 proposed by Horpibulsuk and Miura (2001) was used to characterise the nonlinear stress-strain behaviour of the
 231 fibre-reinforced clay.

232 In order to consider the nonlinear behaviour (i.e., strain hardening/softening) of the effective stress ratio and deviator
 233 stress of the fibre-reinforced clay, the variation of the effective stress ratio and deviator stress of the fibre-reinforced
 234 soil with the axial strain in terms of modified hyperbolic relation takes the following forms:

$$235 \quad \frac{q}{p'} = \frac{\varepsilon}{a+b\varepsilon^n} \quad a, b \text{ and } n \text{ are the modified hyperbolic model parameters for effective stress ratio (Eq.4)$$

$$236 \quad q = \frac{\varepsilon}{g+h\varepsilon^t} \quad g, h \text{ and } t \text{ are the modified hyperbolic model parameters for deviator stress} \quad (Eq.5)$$

237 The parametric study of the influence of model parameters on the evolution of effective stress ratio ($\frac{q}{p'}$) and deviator
 238 stress (q) are shown in **Figures 6** and **7**, respectively. **Figure 6** shows that a controlled the value of the initial
 239 tangent to the $q/p' - \varepsilon$ behaviour while b accounted for the residual value and n was responsible for the slope of the
 240 post peak drop of the $q/p' - \varepsilon$ curve.

241 The effective stress ratio and deviator stress data of the consolidated undrained triaxial tests on both unreinforced
 242 and fibre-reinforced soil samples were used to determine the coefficients of the modified hyperbolic model using a
 243 nonlinear regression analysis. **Figures 8 and 9** show the calculated coefficients for both unreinforced and fibre-
 244 reinforced soil samples tested at different initial effective consolidation stresses. The calculated hyperbolic model
 245 parameters for the stress-strain behaviour of the fibre-reinforced samples with different fibre contents and subjected
 246 to different initial effective consolidation stresses showed a nonlinear trend for both ABF and GBF fibres.
 247 Therefore, to develop a set of meaningful correlations between calculated coefficients and the fibre content, the
 248 parameters were further normalised to the values of initial effective consolidation stress and fibre content. The
 249 following equations show the relationships between the normalised coefficients and the initially non-normalised
 250 coefficients used in the modified hyperbolic model. **Figures 10 and 11** depict the relationships between the
 251 normalised parameters and the fibre content.

$$252 \quad a^* = \log\left(\frac{a}{100\sigma'_c}\right)(1 + 100f) = k_{1a} \times f + k_{2a} \quad (\text{Eq.6})$$

$$253 \quad b^* = \log\left(\frac{b}{100}\right)(1 + 100f) = k_{1b} \times f + k_{2b} \quad (\text{Eq.7})$$

$$254 \quad n^* = \text{Exp}(-n)(1 + 100f) = k_{1n} \times f + k_{2n} \quad (\text{Eq.8})$$

$$255 \quad g^* = \log\left(\frac{\sigma'_c g^2}{100}\right)(1 + 100f) = k_{1g} \times f + k_{2g} \quad (\text{Eq.9})$$

$$256 \quad h^* = \log\left(\frac{\sigma'_c h^2}{100}\right)(1 + 100f) = k_{1h} \times f + k_{2h} \quad (\text{Eq.10})$$

$$257 \quad t^* = \text{Log}(100t)(1 + 100f) = k_{1t} \times f + k_{2t} \quad (\text{Eq.11})$$

258 where; σ'_c stands for the initial effective consolidation stress, f stands for the fibre content and

259 $k_{1a,g}, k_{2a,g}, k_{1b,h}, k_{2b,h}, k_{1n,t}, k_{2n,t}$ are the coefficients of the linear equations (see **Figures 10 and 11**).

260 Therefore, the original coefficients of the modified hyperbolic model can be expressed based on the fibre content,
 261 initial effective consolidation stress and the linear equations presented in **Figures 10 and 11** using **equations 12 to**
 262 **17**.

$$263 \quad a = \sigma'_c 10^{\left(2 + \frac{k_{1a} \times f + k_{2a}}{1 + 100f}\right)} \quad (\text{Eq.12})$$

$$264 \quad b = 10^{\left(2 + \frac{k_{1b} \times f + k_{2b}}{1 + 100f}\right)} \quad (\text{Eq.13})$$

$$265 \quad n = -\ln\left(\frac{k_{1n} \times f + k_{2n}}{1 + 100f}\right) \quad (\text{Eq.14})$$

$$266 \quad g = \sqrt{\frac{1}{\sigma'_c} 10^{\left(2 + \frac{k_{1g} \times f + k_{2g}}{1 + 100f}\right)}} \quad (\text{Eq.15})$$

$$267 \quad h = \sqrt{\frac{1}{\sigma'_c} 10^{\left(2 + \frac{k_{1h} \times f + k_{2h}}{1 + 100f}\right)}} \quad (\text{Eq.16})$$

$$268 \quad t = 10^{\left(-2 + \frac{k_{1t} \times f + k_{2t}}{1 + 100f}\right)} \quad (\text{Eq.17})$$

269 Combining **equations 4 and 5** with **equations 12 to 17** results in the following equations for predicting the effective
 270 shear stress ratio and deviator stress of the fibre-reinforced clay:

$$271 \quad \left(\frac{q}{p'}\right)_{re} = \frac{0.01 \times \varepsilon}{\sigma'_c \times 10^{\frac{k_{1a} \times f + k_{2a}}{1+100f}} + 10^{\left(\frac{k_{1b} \times f + k_{2b}}{1+100f}\right) \varepsilon} - \ln\left(\frac{k_{1n} \times f + k_{2n}}{1+100f}\right)} \quad (\text{Eq.18})$$

$$272 \quad q_{re} = \frac{0.01 \times \varepsilon}{\sqrt{\frac{1}{\sigma'_c} 10^{\frac{k_{1g} \times f + k_{2g}}{1+100f}} + \varepsilon^{10^{\left(-2 + \frac{k_{1t} \times f + k_{2t}}{1+100f}\right)}}} \sqrt{\frac{1}{\sigma'_c} 10^{\frac{k_{1h} \times f + k_{2h}}{1+100f}}}} \quad (\text{Eq.19})$$

273 **Equations 18 and 19** can also be rewritten for unreinforced soil (i.e., $f = 0$):

$$274 \quad \left(\frac{q}{p'}\right)_{un} = \frac{0.01 \times \varepsilon}{\sigma'_c \times 10^{k_{2a}} + 10^{k_{2b} \times \varepsilon - \ln(k_{2n})}} \quad (\text{Eq.20})$$

$$275 \quad q_{re} = \frac{0.01 \times \varepsilon}{\sqrt{\frac{1}{\sigma'_c} 10^{k_{2g}} + \varepsilon^{10^{(k_{2t}-2)}}} \sqrt{\frac{1}{\sigma'_c} 10^{k_{2h}}}} \quad (\text{Eq.21})$$

276 **Figure12** compares the predicted data using the developed regression model for the relationships between effective
 277 stress ratio and axial strain of the unreinforced and fibre-reinforced soil samples studied in this research.

4.3. Proposed method to predict the stress ratio of fibre-reinforced clays

278 In this study, the modified hyperbolic model was used to predict the effective stress ratio and deviator stress of the
 279 fibre-reinforced clay for practical application. The model parameters can be calculated using the following steps:

- 280 1) Use **equations 4 and 5** to fit the test data of unreinforced and fibre-reinforced soil samples using nonlinear
 281 regression analysis and determine a, b and n or g, h and t.
- 282 2) Use **equations 6 to 11** to calculate the normalised parameters a*, b* and n* or g*, h* and t*.
- 283 3) Draw the best fit line through the graphs of normalised parameters (calculated in step 2) versus fibre
 284 content to calculate $k_{1a,g}$, $k_{2a,g}$, $k_{1b,h}$, $k_{2b,h}$, $k_{1n,t}$ and $k_{2n,t}$.
- 285 4) Use **equations 18 and 19** to predict the effective stress ratio and deviator stress of the fibre-reinforced clay,
 286 respectively.

287 The model calibration phase as explained above aims to capture the inherent properties of the soil and fibres into the
 288 equation in form of model parameters. Therefore, once the model is calibrated based on a particular clay type and a
 289 particular fibre type, it can predict the effective shear stress ratio and deviator stress of the clay at different axial
 290 strains during the triaxial compression test. The model parameters can be adequately estimated using a minimum of
 291 2 tests on an unreinforced soil (at two different initial effective consolidation stresses) and two tests on fibre-
 292 reinforced clay (with a fibre content at two different initial effective consolidation stresses). A medium range fibre
 293 content is recommended for calibration stage. To increase the accuracy of the model it is recommended to use the
 294 triaxial test data of three unreinforced soil samples tested at different effective consolidation stresses.

4.4. Validation of the model

295 The proposed model was validated by comparing its predictions with some of the published experimental data
 296 available in the literature. The stress-strain data of the chosen research works were extracted by digitising the
 297 reported graphs.

298 Wu et al. (2014) carried out a series of undrained triaxial tests on fibre-reinforced silty clay samples with 0.5%, 1%
299 and 1.5% sisal fibres. They reported a gradual increase in deviator stress of fibre-reinforced soil with an increase in
300 fibre content. However, the rate of deviator stress improvement was declined beyond 1% fibre content. **Figure 13**
301 shows the predicted data using the model introduced in this study. The model parameters were calculated using
302 experimental data of the unreinforced and 1% fibre-reinforced samples tested at consolidation stresses of 100 kPa
303 and 400 kPa, respectively. The developed model in this study could predict the experimental results at 200 kPa
304 consolidation stress for 0.5%, 1% and 1.5% fibre-reinforced clay with 0.5% to 5% underestimation.

305 Babu and Chouksey (2010) also carried out a series of undrained tests on randomly distributed fibre-reinforced clay
306 samples with 0.5%, 1% and 2% coir fibres. The results indicated that the fibre-reinforced soil gained a higher
307 strength than unreinforced soil with the increase in fibre content to the studied limit of 2% fibre content. They also
308 developed an analytical model based on Cam Clay model to predict the shear strength of fibre-reinforced soil.
309 Although their model fitted well with the experimental results, they did not validate their model with published data.
310 **Figure 14** shows the experimental results reported in their article and the predicted data using the proposed model in
311 this study. The model parameters were acquired from triaxial test data carried out on unreinforced and 1% fibre-
312 reinforced soil at consolidation stresses of 50 and 150 kPa, respectively. According to **Figure 14**, the ratios of the
313 effective stress ratio of 0.5%, 1% and 2% coir fibre-reinforced clay predicted by the developed model in this study
314 to that of the experimental results at consolidations stress of 100 kPa at 12% axial strain were 1.03, 0.99 and 0.95,
315 respectively.

316 Ozkul and Baykal (2007) reported an increase in drained and undrained deviator stress of saturated silty clay
317 reinforced with 10% short tyre buffing fibres. They also determined a limiting confining pressure of 200-300 kPa
318 beyond which the presence of rubber fibres reduced the shear strength of the soil. The undrained experimental data
319 reported by Ozkul and Baykal (2007) was used to validate the model developed in this study. Therefore, the model
320 parameters were calculated using the test data of unreinforced soil at consolidation stresses of 100 kPa and 300 kPa
321 in addition to the single test data of fibre-reinforced soil at consolidation stress of 300 kPa. **Figure 15** shows the
322 experimental data and predicted deviator stress curves. The ratios of the deviator stresses of 10% rubber fibre-
323 reinforced clay predicted by the developed model in this study to that of the experimental results at consolidation
324 stresses of 100 kPa, 200 kPa and 300 kPa at 12% axial strain were 1.04, 0.97 and 0.99, respectively.

325 In another study, Nguyen and Fatahi (2016) reported the mechanical behaviour of fibre-reinforced cemented clay
326 with polypropylene fibres using a series of consolidated undrained triaxial tests. They also developed a constitutive
327 model called C3F based on Modified Cam Clay (MCC) model to predict the shear strength of fibre-reinforced clays
328 with and without cementation. Their model could predict the shear strength of the fibre-reinforced cemented clay in
329 a good agreement with the experimental results. **Figure 16** shows the undrained experimental results on fibre-
330 reinforced clay samples stabilised with 15% cemented, predicted results using C3F model and also the predicted test
331 data using the method introduced in this study. The model parameters were acquired using data of unreinforced and
332 0.5% fibre-reinforced soil tested at effective consolidation stresses of 400 kPa and 800 kPa, respectively. According
333 to **Figure 16**, at consolidation stress of 200 kPa and 12% axial strain the developed model in this study

334 overestimated the deviator stress of 0.3% and 0.5% fibre-reinforced soil by 4% and 15% respectively and the C3F
335 model underestimated both by 4%. However, at 800 kPa consolidation stress and 12% axial strain, the developed
336 model in this study and C3F model overestimated the deviator stress of 0.3% and 0.5% fibre-reinforced soil both by
337 the same values of 16% and 10%, respectively.

338 Khatri et al. (2016) also carried out a series of undrained triaxial tests on fibre-reinforced clay with 0.4% to 1.6%
339 coir fibre. They reported that the shear strength of fibre-reinforced clay was improved with the increase in fibre
340 content and developed a successful hyperbolic model to predict their own data. However, they did not correlate the
341 model parameters with fibre content or consolidation stress and their model was not validated against available data
342 in the literature. **Figure 17** compares the experimental data and those predicted by the developed model in this
343 study. The model parameters were calculated using experimental data of unreinforced and 0.8% fibre-reinforced soil
344 at consolidation stresses of 77.48 kPa and 313.92 kPa, respectively. The developed model in this study
345 underestimated the effective stress ratio of the 0.4%, 0.8% and 1.6% fibre-reinforced soil at consolidation stress of
346 77.48 kPa and 12% axial strain by 10%, 10% and 3%, respectively. However, at consolidation stress of 313.92 kPa
347 and 12% axial strain, the effective stress ratio of 0.4%, 0.8% and 1.6% fibre-reinforced soil was overestimated by
348 18%, 1% and 5%, respectively.

349 **Table 3** demonstrates a comparison of experimental and predicted results of above-studied research works. The
350 developed nonlinear regression model based on the modified hyperbolic model and the proposed technique to
351 acquire the model parameters in this study could capture the experimental stress-strain results reasonably well
352 considering the less effort to calculate the model parameters compared to using constitutive models.

353 The **Supplemental Material** for this article explains the technique to calculate the model parameters for the
354 modified hyperbolic model based on the triaxial test results reported by **Wu et al. (2014)**.

5. Conclusions

355 In this research, the shear strength behaviour of a clay reinforced with two types of carpet waste fibre was
356 investigated by conducting a set of consolidated undrained triaxial shear tests on fibre-reinforced samples with 1%,
357 3% and 5% fibre contents. The fibre-reinforced soils exhibited significant variation in the Proctor compaction curve
358 to that of the unreinforced soil. Therefore, to eliminate the effect of initial unit weight on the stress-strain results, all
359 samples were prepared at an identical dry unit weight (i.e., 17.8 kN/m³) and their respective moisture contents based
360 on the standard Proctor compaction curves for the unreinforced and fibre-reinforced soils.

361 Fibre reinforcement using waste carpet fibres improved the stress-strain behaviour of the clay significantly and the
362 contribution of the fibres to increase the effective stress ratio and deviator stress of the soil increased with fibre
363 content. At higher initial effective consolidation stresses prior to the shearing stage, fibres stretch increasingly and
364 therefore, contribute better to distribute the disturbing shear stresses into a wider area upon initiating the shear stage.
365 However, at lower initial effective consolidation stresses, fibres cannot stretch effectively and may slip during the
366 shear. Hence, fibres may not confine soil grains and add surplus strength to the reinforced soil. Therefore, increase
367 in fibre content at a low initial effective consolidation stress may have an insignificant effect on the shear strength of

368 the fibre-reinforced soil without necessary soil grain harnessing effect. Increase in fibre content results in changing
369 the stress-strain behaviour of the unreinforced soil sample to a strain hardening behaviour. This research indicated
370 that up to 5% carpet waste fibre could be optimally used for improving the shear strength behaviour of clay and
371 hence introduces carpet waste fibres as sustainable soil reinforcing materials to improve the shear strength of weak
372 soils.

373 Two nonlinear regression models were developed based on the modified hyperbolic model to predict the effective
374 stress ratio and deviator stress of the fibre-reinforced clay. The model parameters can be determined from the
375 triaxial test results on unreinforced and a fibre-reinforced soil sample at two different consolidation stresses. The
376 model can predict the stress-strain curve of the fibre-reinforced clay with knowing the initial effective consolidation
377 stress and the fibre content. The model was verified with the available data in the literature and predictions by the
378 model agreed reasonably well with the published experimental data. The proposed model is relatively simple
379 compared to other developed regression models and constitutive models reported in the literature in that it eliminates
380 the requirement for advanced soil testing and knowledge of fibre properties. This model can be used as a tool to
381 predict the shear strength of fibre-reinforced clay in geotechnical engineering practice with limited knowledge of the
382 soil properties and less number of testing.

383 **Acknowledgements**

384 The authors wish to express their gratitude to Envirolink Northwest (United Kingdom) for funding part of this
385 project, Carpet Recycling UK and Milliken Industries for supplying the fibres. The fourth author is grateful to a
386 financial support from Suranaree University of Technology and the Thailand Research Fund under the TRF Senior
387 Research Scholar program Grant No. RTA5980005.
388

389 **References**

- 390 Ahmad, F., Bateni, F., Azmi, M. (2010). "Performance evaluation of silty sand reinforced with fibres." *J. of*
391 *Geotex. and Geomem.*, 28(1), 93-99.
- 392 Al-Akhras, N. M., Attom, M. F., Al-Akhras, K. M., Malkawi, A. I. H. (2008). "Influence of fibers on swelling
393 properties of clayey soil." *Geosynthetics Int. J.*, 15(4), 304-309.
- 394 Ang, E. C., Loehr, J. E. (2003). "Specimen size effects for fiber-reinforced silty clay in unconfined compression"
395 *Geotechnical Testing Journal* 26(2), 1-10.
- 396 Anggraini, V., Asadi, A., Farzadnia, N., Jahangirian, H., Huat, B. B. K. (2016). "Effects of coir fibres modified
397 with Ca(OH)₂ and Mg(OH)₂ nanoparticles on mechanical properties of lime-treated marine clay." *Geosynthetics*
398 *Int. J.*, 23(3), 206-218.
- 399 Babu, G. L. S., and Chouksey, S. K. (2010). "Model for analysis of fiber-reinforced clayey soil." *Geomech.*
400 *Geoeng.*, 5(4), 277-285.
- 401 Babu, G. L.S., Vasudevan, A. K. (2008). "Strength and stiffness response of coir fiber-reinforced tropical soil." *J. of*
402 *Mat. in Civil Eng.*, 20(9), 571-577.
- 403 Botero, E., Ossa, A., Sherwell, G., and Ovando-Shelley, E. (2015). "Stress-strain behavior of a silty soil reinforced
404 with polyethylene terephthalate (PET)." *J. of Geotex. and Geomem.*, 43(4), 363-369.
- 405 British Standards Institution. 1990. BS 1377: Part 8: 1990 British Standard Methods of test for Soils for civil
406 engineering purposes-Part 8. Shear strength tests (effective stress). British Standards Institution. United
407 Kingdom.
- 408 Chen, C. W., and Loehr, J. E. (2009). "Undrained and drained triaxial tests of fiberreinforced sand." *Geosynthetics*
409 *in Civil and Environmental Engineering*, 114-120.
- 410 Chen, C. W. (2007). "A constitutive model for fiber-reinforced soil." Ph.D. thesis, Univ. of Missouri, Colombia,
411 USA.
- 412 Casagrande, M.D.T., Coop, M.R., Consoli, N. (2006). "Behavior of a Fiber-Reinforced Bentonite at Large Shear
413 Displacements." *J. of Geotech. Geoenviron. Eng.*, 132(11), 1505-1508.
- 414 Consoli, N.C., Casagrande, M.D.T., Coop, M.R. (2007). "Performance of fibre-reinforced sand at large shear
415 strains." *Geotechnique*, 57(9), 751-756.
- 416 Diambra A., Ibraim E., Wood M., Russell A. (2010). "Fiber reinforced sands: experiments and modelling." *J. of*
417 *Geotex. and Geomem.*, 28, 238-50.
- 418 Diambra, A., Russell, A. R., Ibraim, E. and Muir Wood, D. (2007). "Determination of fibre orientation distribution
419 in reinforced sand." *Geotechnique*, 57(7), 623-628.
- 420 Diambra, A., Ibraim, E. (2014). "Modelling of fibre cohesive soil mixtures." *Acta Geotech.*, 9, 1029-1043.

- 421 Duncan, J.M. and Chang, C.Y. (1970). "Nonlinear analysis of stress and strain in soils." *J. of Soil Mechanics &*
 422 *Foundations Div.*, 96(5), 1629-1653.
- 423 Ekinci, A., and Ferreira, P. (2012). "The undrained mechanical behavior of fiber reinforced heavily over-
 424 consolidated clay", TC 211 - International symposium on Recent Research, Advances & Execution Aspects of
 425 Ground Improvement works, Brussels, Belgium, 53-62.
- 426 Falorca, I. M.C.F.G., Pinto, M. I.M. and Ferreira, G. L. M. (2006). "Residual shear strength of sandy clay reinforced
 427 with short polypropylene fibers randomly oriented." In: *Proceeding of 8th int. conf. on geosynt. (8ICG)*,
 428 Yokohama, 4, 1663-1666.
- 429 Fatahi, B., Fatahi, B., Le, T. M., and Khabbaz, H. (2013a). "Small-strain properties of soft clay treated with fibre
 430 and cement." *Geosynthetics Int.*, 20(4), 286-300.
- 431 Fatahi, B., Khabbaz, H. & Fatahi, B. (2012). "Mechanical characteristics of soft clay treated with fibre and cement."
 432 *Geosynthetics Int. J.*, 19(3), 252-262.
- 433 Fatahi, B., Le, T. M., Fatahi, B., and Khabbaz, H. (2013b). "Shrinkage properties of soft clay treated with cement
 434 and geofibers." *Geotech. Geol. Eng. J.*, 31(5), 1421-1435.
- 435 Freilich, B.J., Li, C. and Zornberg, J.G. (2010). "Effective shear strength of fiber-reinforced clays." In *9th*
 436 *International Conference on Geosynthetics, Brazil, 1997-2000*.
- 437 Ghiassian, H., Poorebrahim, G. and Gray, D. (2004). "Soil Reinforcement with Recycled Carpet Wastes.", *Waste*
 438 *Management & Research J.*, 22, 108-114.
- 439 Gray, D.H. and Ohashi, H. (1983). "Mechanics of Fiber Reinforced in Sand." *Journal of Geotec. and Geoenv. Eng.*,
 440 109(3), 335-353.
- 441 Hamidi, A., Hooresfand, M. (2013). "Effect of fiber reinforcement on triaxial shear behavior of cement treated
 442 sand." *J. of Geotex. and Geomem.*, 36,1-9.
- 443 Horpibulsuk, S., and Miura, N. (2001). "Modified hyperbolic stress-strain response: uncemented and cement
 444 stabilized clays", Report of the Faculty of Science and Engineering, Saga University, Japan, 30(1), 39-47.
- 445 Horpibulsuk, S. and Rachan, R. (2004), "Modified hyperbolic model for capturing undrained shear behavior."
 446 *Lowland Technology International*, 6(2), 11-20.
- 447 Jamsawang, P., Voottipruex, P. and Horpibulsuk, S. (2015), "Flexural strength characteristics of compacted-cement-
 448 polypropylene fiber-sand" *J. of Mat. in Civil Eng.*, 27(9), 04014243(1-9).
- 449 Khatri, V. N., Dutta, R. K., Venkataraman, G., & Shrivastava, R. (2016). "Shear Strength Behaviour of Clay
 450 Reinforced with Treated Coir Fibres." *Periodica Polytechnica. Civil Eng.*, 60(2), 135-143.
- 451 Lambe, T. W., and Whitman, R. V. (1979), "Soil Mechanics," 2d ed., John Wiley & Sons, Inc., New York, USA.
- 452 Maher, M.H., Gray, D.H. (1990). "Static response of sands reinforced with randomly distributed fibers." *J. of*

- 453 *Geotech. Eng.*, 116(11), 1661-1677.
- 454 Maliakal, T., and Thiyyakkandi, S. (2013), "Influence of randomly distributed coir fibers on shear strength of clay."
 455 *Geotechnical and Geological Engineering*, 31(2), 425-433.
- 456 Michalowski, R.L. (2008). "Limit analysis with anisotropic fibre-reinforced soil." *Geotechnique*, 58(6), 489-502.
- 457 Michalowski R L, Zhao A. (1996). "Failure of fiber-reinforced granular soils." *J. of Geotec. Eng.*, 122(3), 226-234.
- 458 Miranda Pino, L. and Baudet, B. (2015). "The effect of the particle size distribution on the mechanics of fibre-
 459 reinforced sands under one-dimensional compression." *J. of Geotex. and Geomem.* 43 (3), 250-258.
- 460 Mirzababaei, M., Miraftab, M., Mohamed, M. and McMahon, P. (2013a). "Impact of waste carpet fibres on swelling
 461 properties of compacted clays." *J. of Geotech. and Geolo. Eng.*, 31(1), 173-182.
- 462 Mirzababaei, M., Miraftab, M., Mohamed, M. and McMahon, P. (2013b). "Unconfined Compression Strength of
 463 Reinforced Clays with Carpet Waste Fibers." *J. of Geotech. Geoenviron. Eng.*, 139(3), 483-493.
- 464 Mirzababaei, M., Arulrajah, A., Horpibulsuk, S., and Aldava, M. (2017a). "Shear strength of a fibre-reinforced clay
 465 at large shear displacement when subjected to different stress histories." *Geotextiles and Geomembranes*,
 466 <https://doi.org/10.1016/j.geotexmem.2017.06.002>.
- 467 Mirzababaei, M., Mohamed, M., and Miraftab, M. (2017b). "Analysis of strip footings on fiber-reinforced slopes
 468 with the aid of particle image velocimetry." *Journal of Materials in Civil Engineering*, 29(4),
 469 [https://doi.org/10.1061/\(ASCE\)MT.1943-5533.0001758](https://doi.org/10.1061/(ASCE)MT.1943-5533.0001758).
- 470 Murray, J. J.; Frost, J. D. and Wang, Y. (2000). "Behavior of a sandy silt reinforced with discontinuous recycled
 471 fiber inclusions." *Transportation Research Record Journal*, 1714, 9-17.
- 472 Nataraj, M.S. and McManis, K.L. (1997). "Strength and Deformation Properties of Soils Reinforced With Fibrillated
 473 Fibers." *Geosynthetics Int. J.*, 4(1), 65-79.
- 474 Newcomb, D. E., Birgisson, B. (1999). "Measuring In Situ Mechanical Properties of Pavement Subgrade Soils."
 475 National Cooperative Highway Research Program, Project 20-5FYA 1996, Washington, USA.
- 476 Nguyen, L., Fatahi, B. (2016). "Behaviour of clay treated with cement & fibre while capturing cementation
 477 degradation and fibre failure – C3F Model" *Int. J. of Plasticity*, 81, 168-195.
- 478 Özkul, Z.H. and Baykal, G. (2007). "Shear behavior of compacted rubber fiber-clay composite in drained and
 479 undrained loading." *J. of geotechnical and Geoenvironmental engineering*, 133(7), 767-781.
- 480 Ranjan, G., Vasan, R. M., Charan, H. D. (1996). "Probabilistic analysis of randomly distributed fiber-reinforced
 481 soil." *J. of Geotech. Eng.*, 122(6), 419-426.
- 482 Sadeghi, M., M., Beigi, F. H. (2014). "Dynamic behavior of reinforced clayey sand under cyclic loading." *J. of*
 483 *Geotex. and Geomem.*, 42(5), 564-572.

- 484 Shukla, S. K., Shivakugan, N., Singh, A. K. (2010). “Analytical model for fiber-reinforced granular soil under high
 485 confining stress.” *J. of Mat. in Civil Eng.*, 22(9), 935-942.
- 486 Waldron, L. J. (1977). “The shear resistance of root permeated homogeneous and stratified soil.” *Soil Science
 487 Society of America Proceedings*, 41, 843-849.
- 488 Wu, Y., Li, Y. and Niu, B. (2014). “Assessment of the mechanical properties of sisal fiber-reinforced silty clay
 489 using triaxial shear tests.” *The Scientific World Journal*, 2014, 436231.
- 490 Özkul, Z.H. and Baykal, G. (2007). ” Shear behavior of compacted rubber fiber-clay composite in drained and
 491 undrained loading.” *J. of geotechnical and Geoenvironmental engineering*, 133(7), 767-781.
- 492 Xiao, H.W., Yannick, N.C.H., Lee, F.H., Zhang, M.H., Ahmad B.S. (2014). “Size effect study on fibre-reinforced
 493 cement-treated clay” *Proceedings of the International Symposium on Geomechanics and Geotechnics: From
 494 Micro to Macro*, Cambridge, U.K., 1351 -1356.
- 495 Zornberg., J. G. (2002). “Discrete framework for limit equilibrium analysis of fibre-reinforced soil.” *Geotechnique*,
 496 52(8), 593-604.

497 **List of Figures:**

- 498 **Figure 1.** Standard Proctor compaction curves of fibre-reinforced clays
- 499 **Figure 2.** Effective stress ratio a) and deviatoric stress b) behaviours of GBF fibre-reinforced clay
- 500 **Figure 3.** Effective stress ratio a) and deviatoric stress b) behaviours of ABF fibre-reinforced clay
- 501 **Figure 4.** Results of repeated test on 5% ABF fibre-reinforced clay
- 502 **Figure 5.** The relationship between deviator stress change ratio and mean effective stress change ratio of fibre-
 503 reinforced clays
- 504 **Figure 6.** Parametric study of the modified hyperbolic model parameters on the effective stress ratio of the soil: the
 505 effect of a) parameter ‘a’ b) parameter ‘b’ c) parameter ‘n’ on the modified hyperbolic function
- 506 **Figure 7.** Parametric study of the modified hyperbolic model parameters on the deviatoric stress of the soil: the
 507 effect of a) parameter ‘g’ b) parameter ‘h’ c) parameter ‘t’ on the modified hyperbolic function
- 508 **Figure 8.** Modified hyperbolic model parameters for $q/p' - \varepsilon$ behaviour of the fibre-reinforced soil samples
- 509 **Figure 9.** Modified hyperbolic model parameters for $q - \varepsilon$ behaviour of the fibre-reinforced soil samples
- 510 **Figure 10.** Normalised modified hyperbolic model parameters for $q/p' - \varepsilon$ behaviour of the fibre-reinforced soil
 511 samples: a,b,c) ABF fibre-reinforced soils d,e,f) GBF fibre-reinforced soils
- 512 **Figure 11.** Normalised modified hyperbolic model parameters for $q - \varepsilon$ behaviour of the fibre-reinforced soil
 513 samples: a,b,c) ABF fibre-reinforced soils d,e,f) GBF fibre-reinforced soils
- 514 **Figure 12.** Experimental and predicted data for effective stress ratio-axial strain response of: (a) GBF fibre-
 515 reinforced soil (b) ABF fibre-reinforced soil
- 516 **Figure 13.** Experimental and predicted data for shear strength response of fibre-reinforced soil (Wu et al., 2014)
- 517 **Figure 14.** Experimental and predicted data for shear strength response of fibre-reinforced soil (Babu and Chouksey,
 518 2010)

519 **Figure 15.** Experimental and predicted data for shear strength response of fibre-reinforced soil (Ozkul and Baykal,
520 2007)

521 **Figure 16.** Experimental and predicted data for shear strength response of fibre-reinforced soil (Nguyen and Fatahi
522 2016)

523 **Figure 17.** Experimental and predicted data for shear strength response of fibre-reinforced soil (Khatri et al., 2016

524 **List of Tables:**

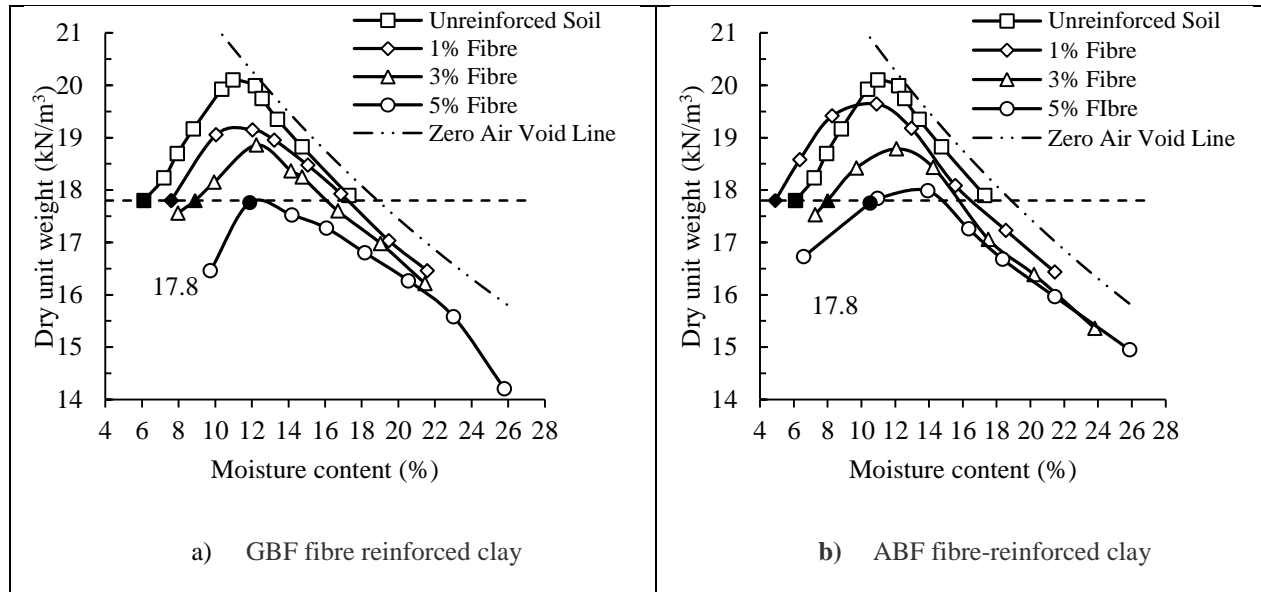
525 **Table 1.** Soil Properties

526 **Table 2.** Properties of carpet waste fibres

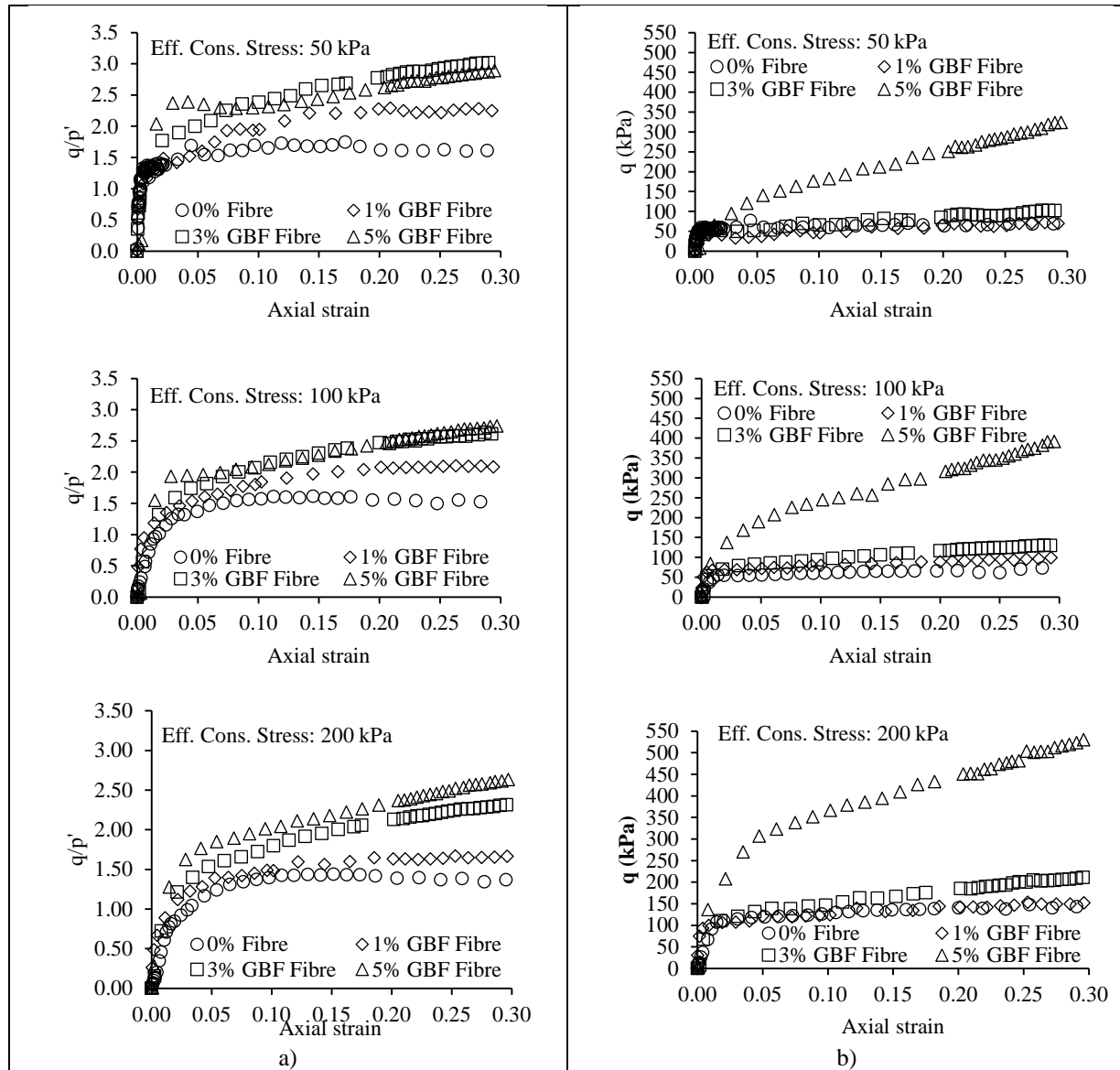
527 **Table 3.** Comparison of experimental and predicted shear strength results

528

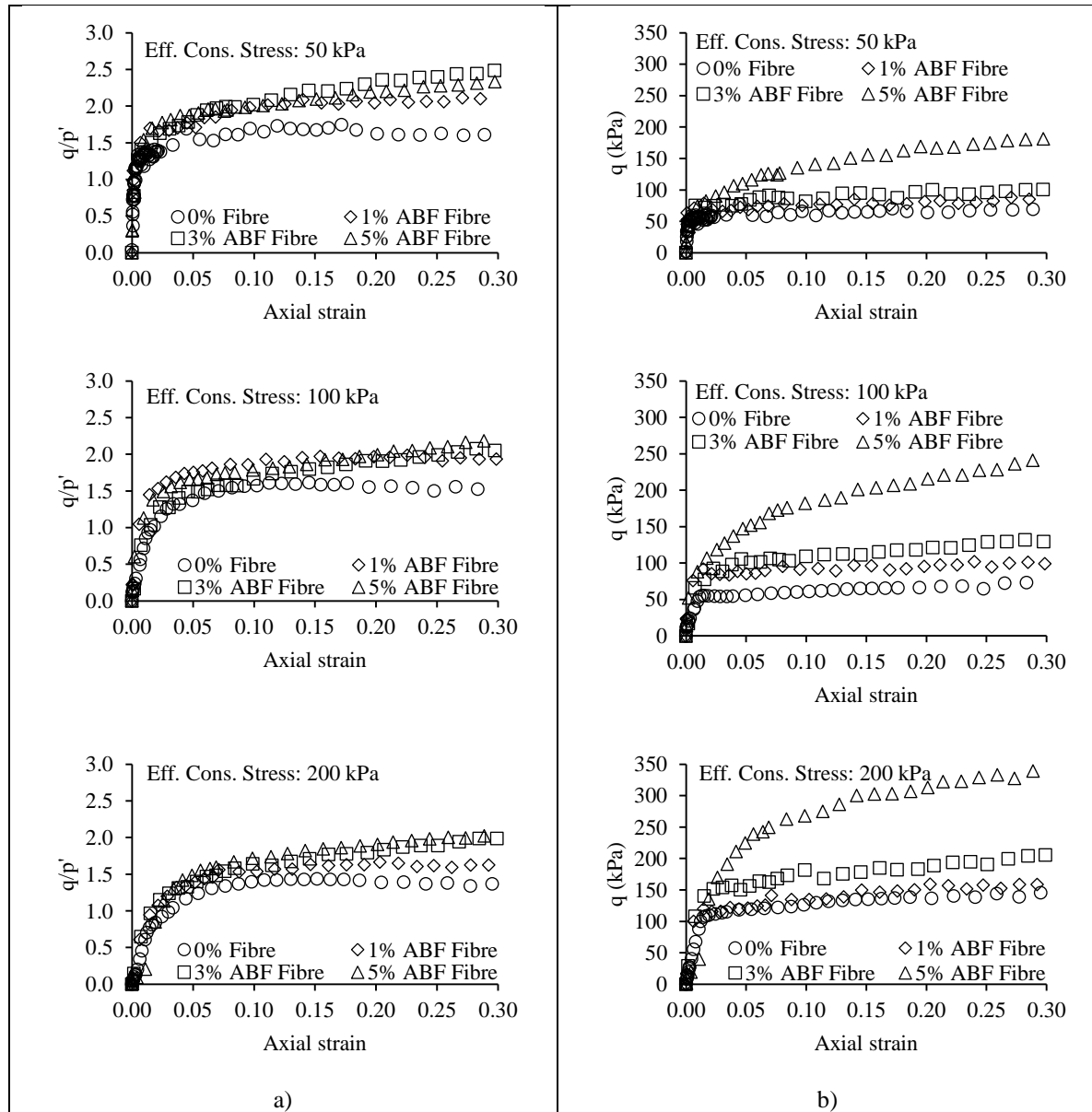
529



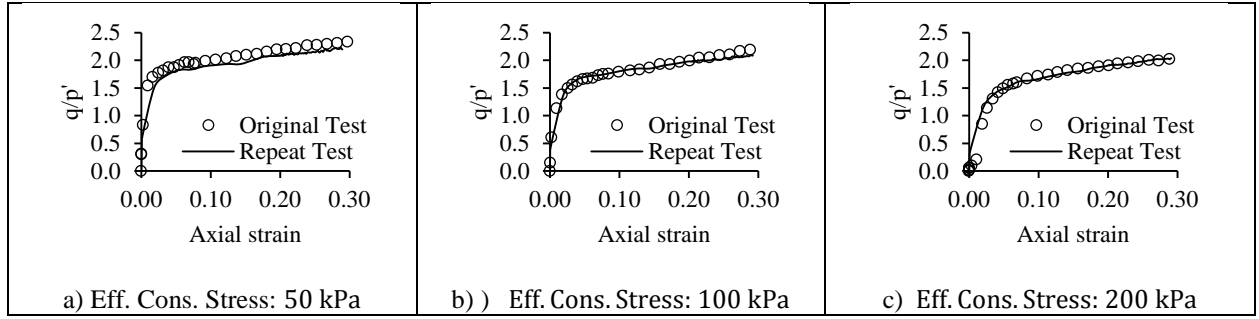
530 Figure 1. Standard Proctor compaction curves of fibre-reinforced clays



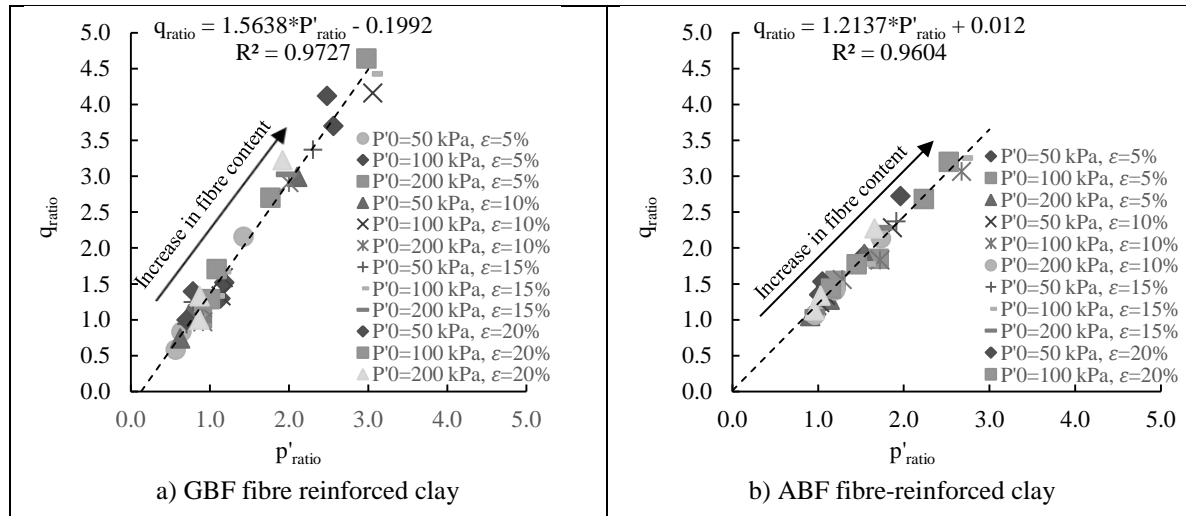
531 Figure 2. Effective stress ratio a) and deviatoric stress b) behaviours of GBF fibre-reinforced clay



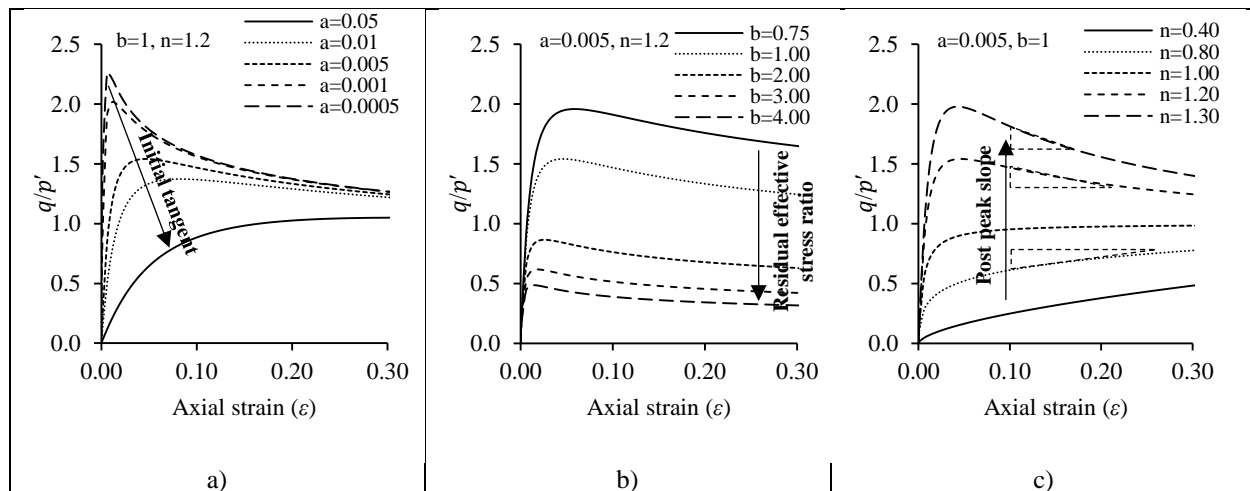
532 Figure 3. Effective stress ratio a) and deviatoric stress b) behaviours of ABF fibre-reinforced clay



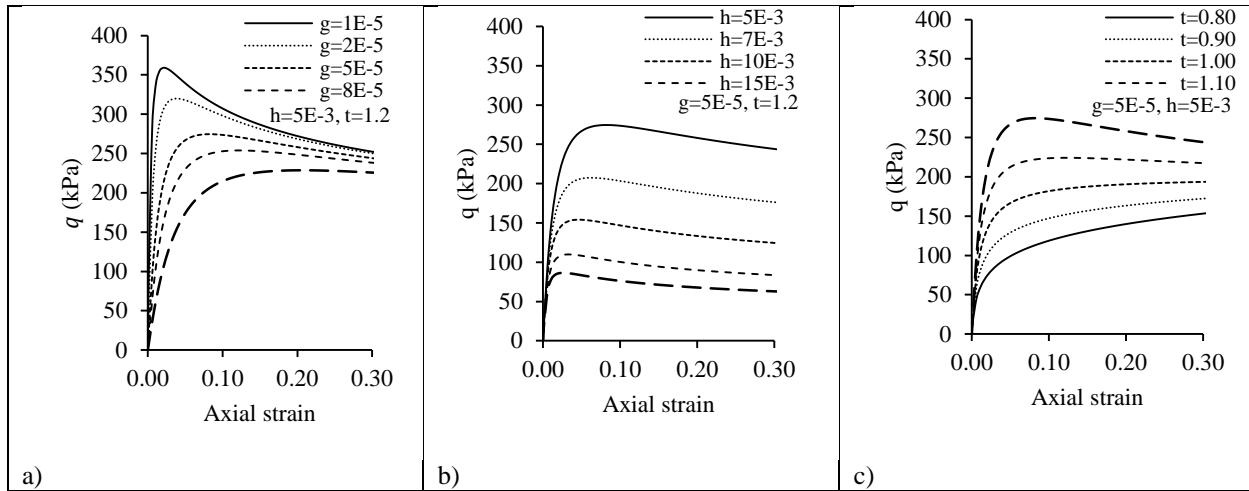
533 Figure 4. Results of repeated tests on 5% ABF fibre-reinforced clay



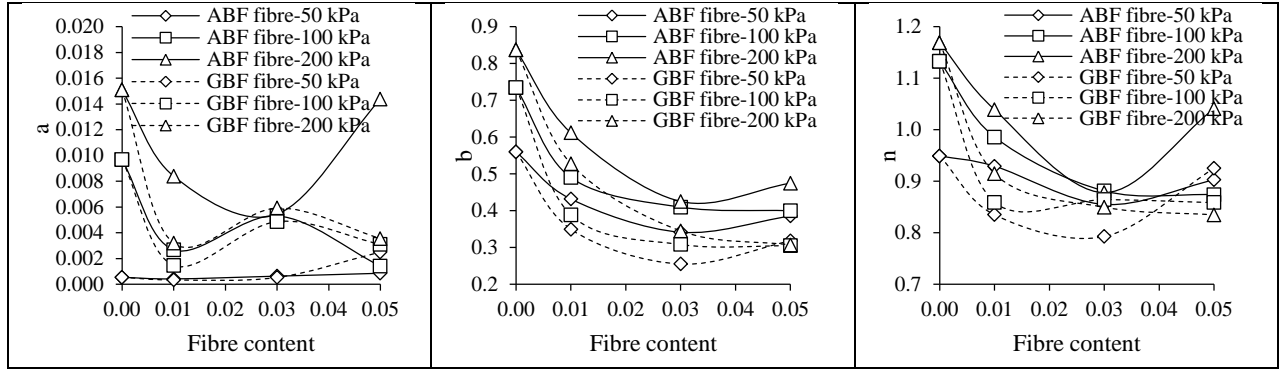
534 Figure 5. The relationship between deviator stress change ratio and mean effective stress change ratio of fibre-
 535 reinforced clays



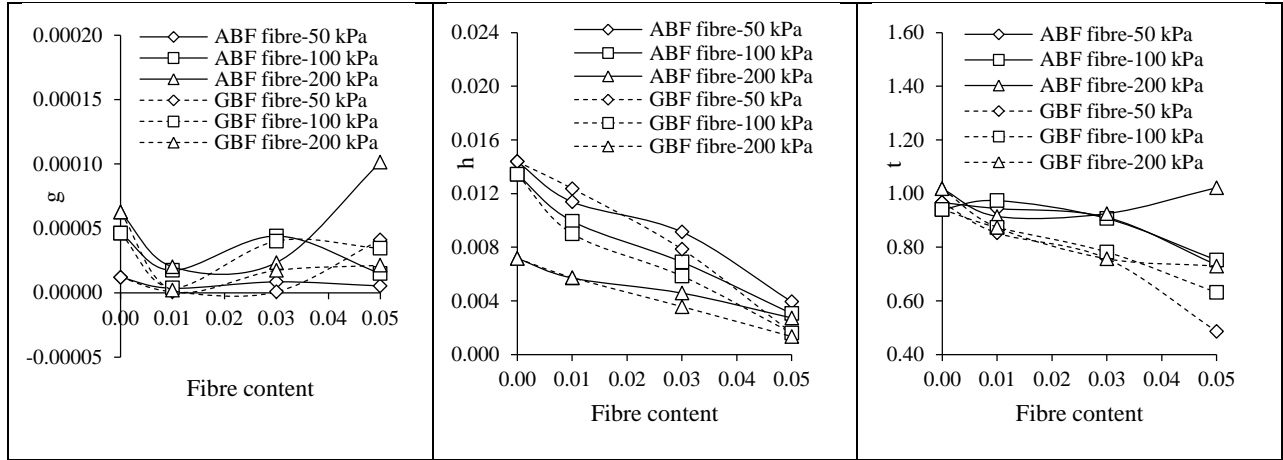
536 Figure 6. Parametric study of the modified hyperbolic model parameters on the effective stress ratio of the soil: the
 537 effect of a) parameter 'a' b) parameter 'b' c) parameter 'n' on the modified hyperbolic function



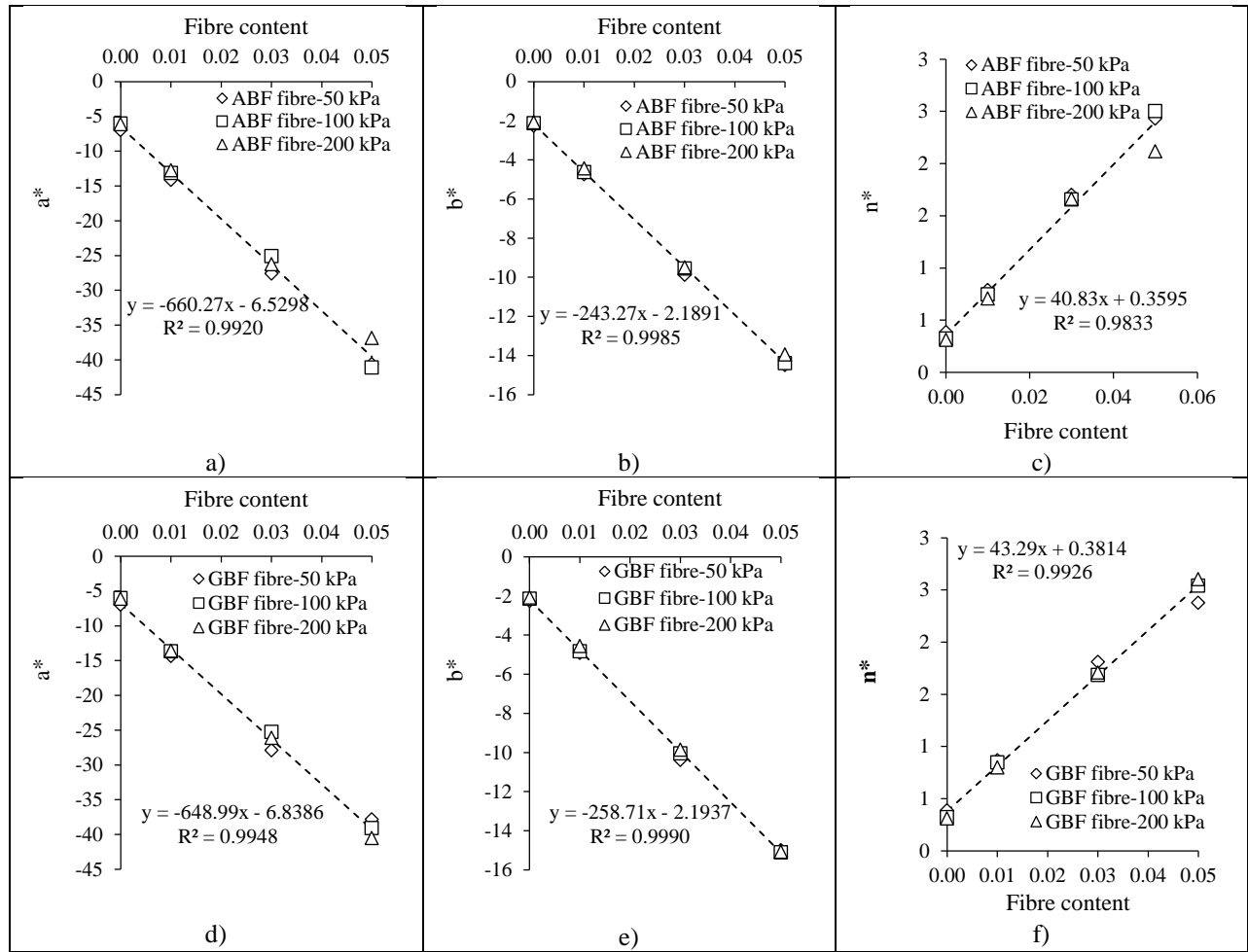
538 Figure 7. Parametric study of the modified hyperbolic model parameters on the deviatoric stress of the soil: the
 539 effect of a) parameter 'g' b) parameter 'h' c) parameter 't' on the modified hyperbolic function



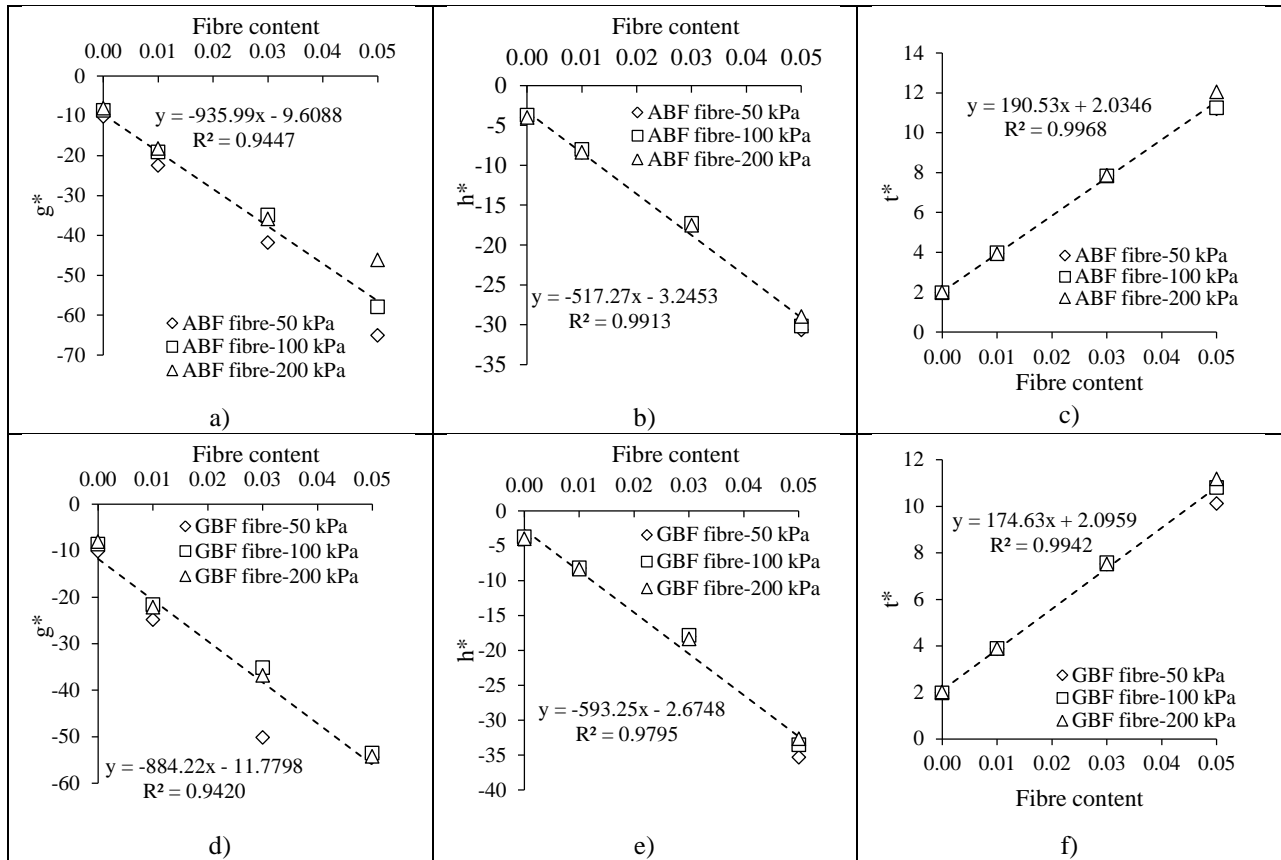
540 Figure 8. Modified hyperbolic model parameters for $q/p' - \varepsilon$ behaviour of the fibre-reinforced soil samples



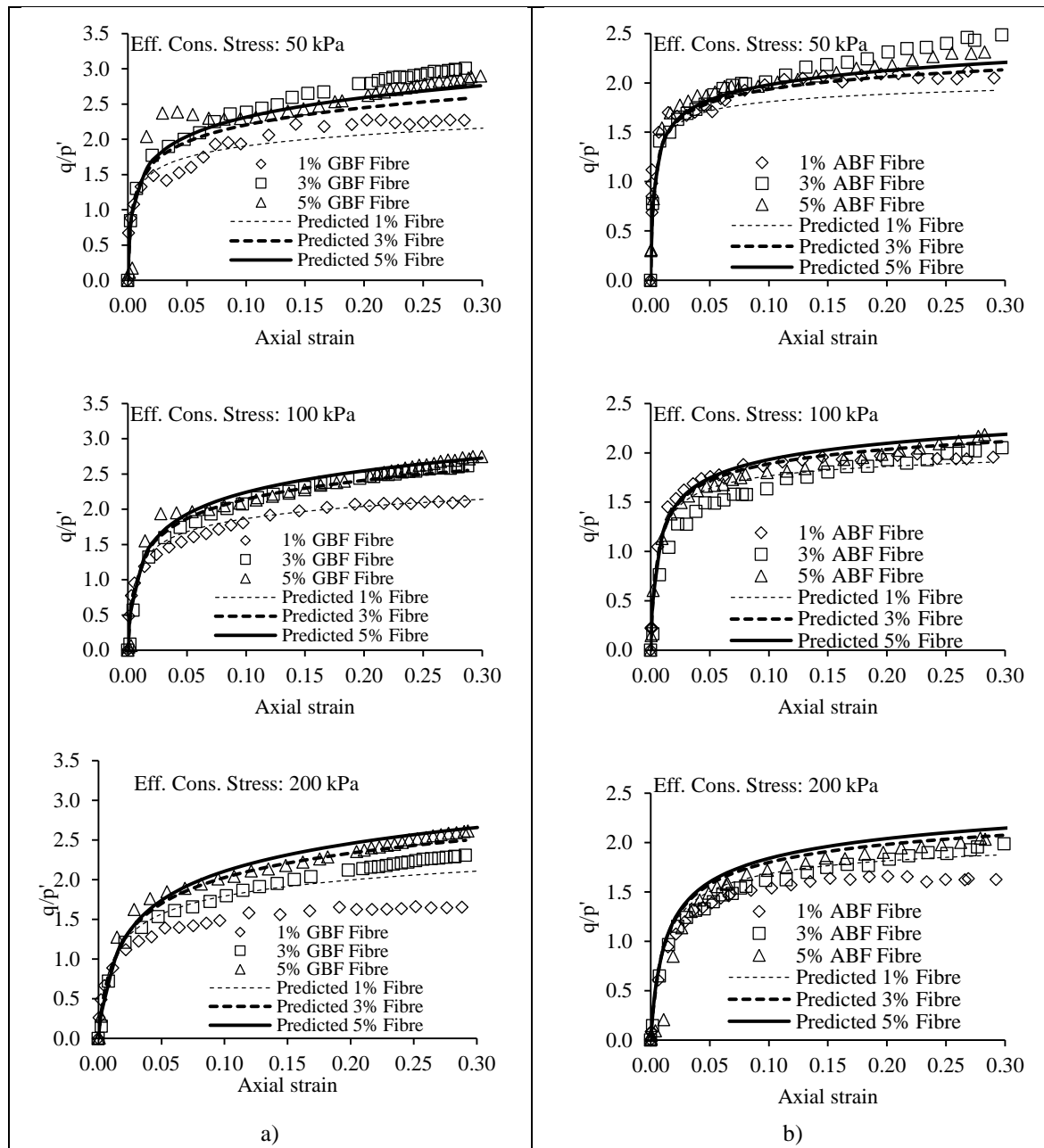
541 Figure 9. Modified hyperbolic model parameters for $q - \epsilon$ behaviour of the fibre-reinforced soil sample



542 Figure 10. Normalised modified hyperbolic model parameters for $q/p' - \varepsilon$ behaviour of the fibre-reinforced soil
 543 samples: a,b,c) ABF fibre-reinforced soils d,e,f) GBF fibre-reinforced soils

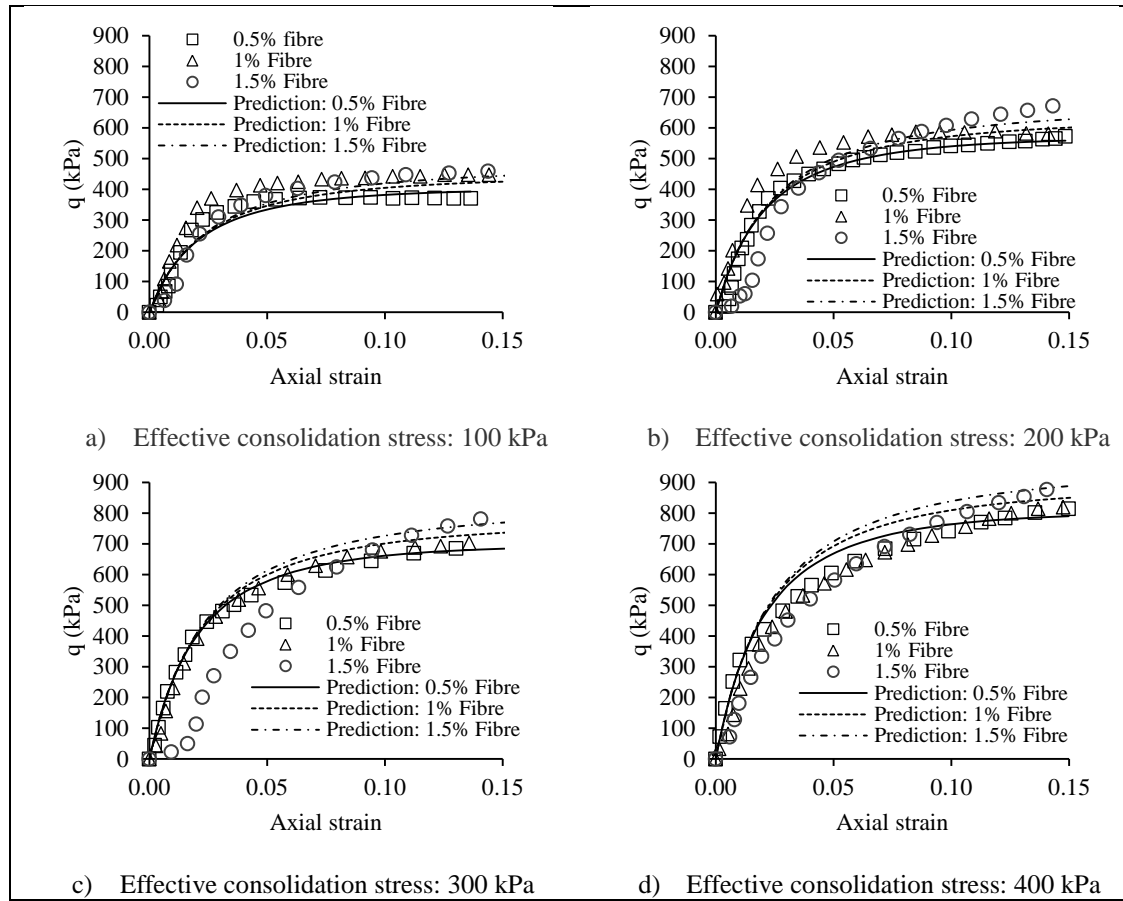


544 Figure 11. Normalised modified hyperbolic model parameters for $q - \epsilon$ behaviour of the fibre-reinforced soil
 545 samples: a,b,c) ABF fibre-reinforced soils d,e,f) GBF fibre-reinforced soils

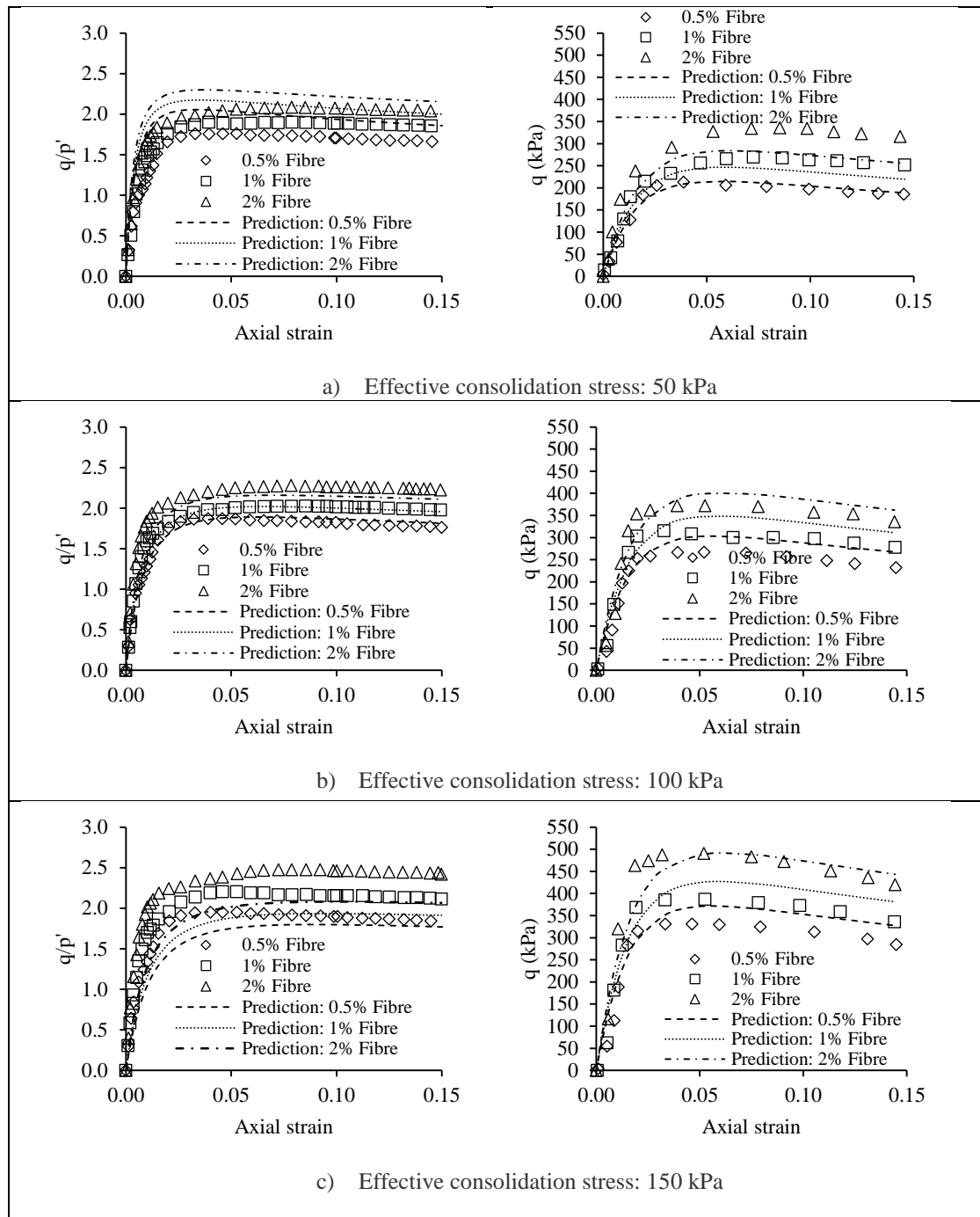


546 Figure 12. Experimental and predicted data for effective stress ratio-axial strain response of:

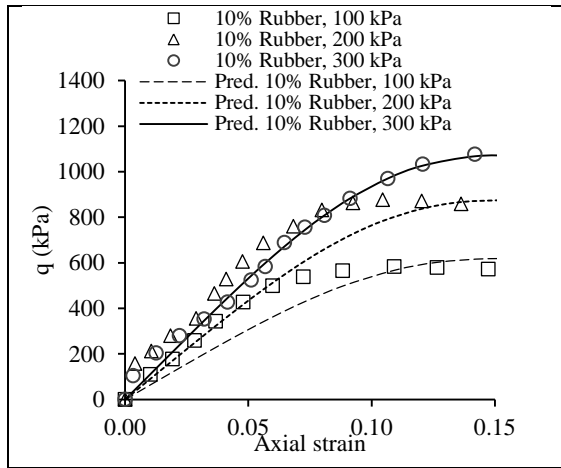
547 a) GBF fibre-reinforced soil b) ABF fibre-reinforced soil



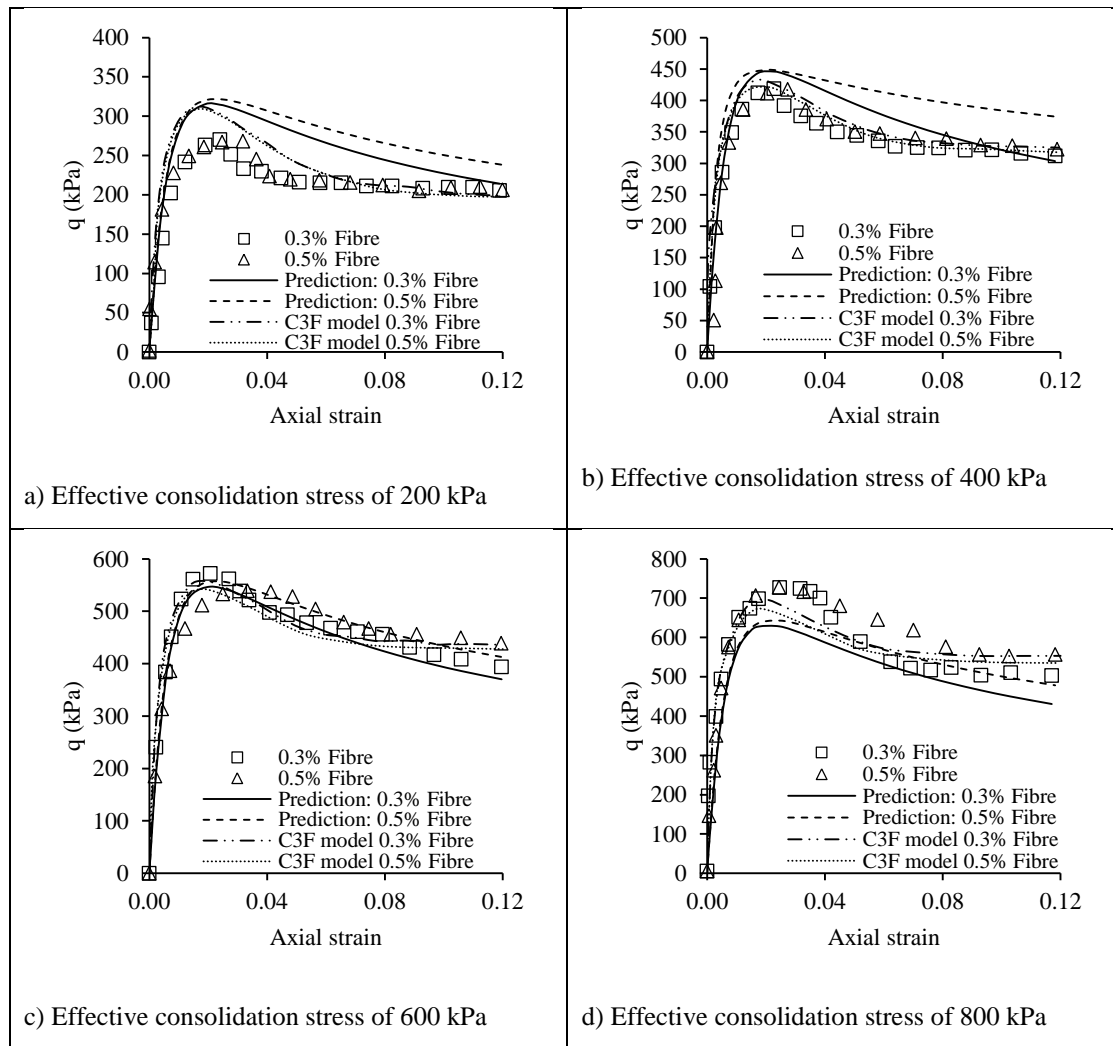
548 Figure 13. Experimental and predicted data for shear strength response of fibre-reinforced soil (Wu et al. 2014)



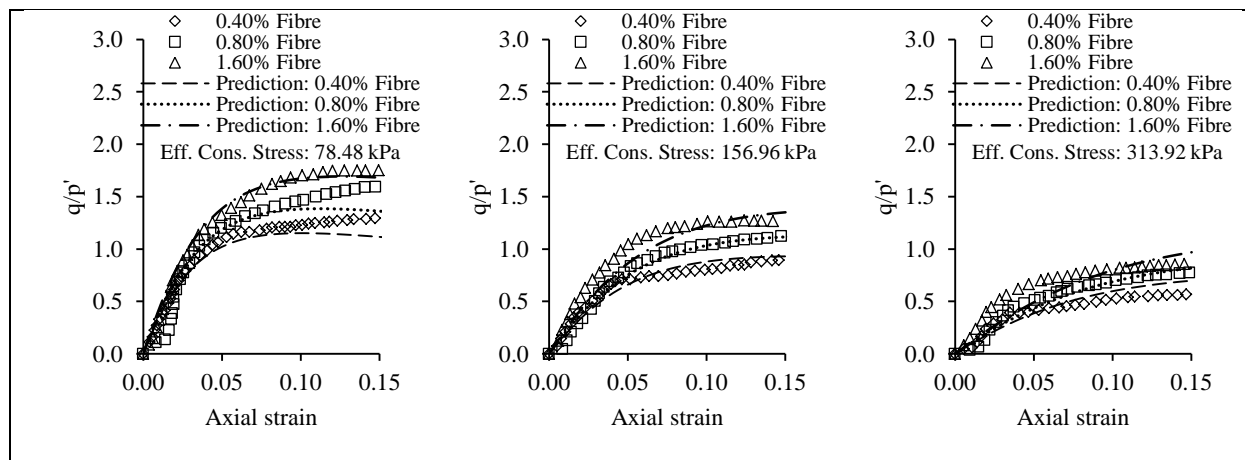
549 Figure 14. Experimental and predicted data for shear strength response of fibre-reinforced soil
 550 (Babu and Chouksey 2010)



551 Figure 15. Experimental and predicted data for shear strength response of fibre-reinforced soil
552 (Ozkul and Baykal 2007)



553 Figure 16. Experimental and predicted data for shear strength response of fibre-reinforced soil
 554 (Nguyen and Fatahi 2016)



555 Figure 17. Experimental and predicted data for shear strength response of fibre-reinforced soil (Khatri et al. 2016)

556

Table 1. Soil Properties

Unified soil classification	CL
Specific gravity	2.68
Gravel (%)	1.42
Sand (%)	42.80
Fine content (%)	55.78
Liquid limit (%)	29.00
Plastic Limit (%)	12.00
Plasticity index (%)	17.00
Maximum dry unit weight (kN/m ³)	20.10
Optimum moisture content (%)	11.00
Swelling pressure (kPa)	76.20

557

Table 2. Properties of carpet waste fibres

	Composition	Specific Gravity*	Water Absorption* (%)	Composition (%)	Specific Tensile Modulus* (GPa/gram/cm ³)
GBF fibre	Polypropylene	0.90	0.0	60	0.27~0.44
	Styrene-Butadiene Rubber (SBR)	0.99	-	20	-
	Nylon	1.14	4.1-4.5	15	0.40~0.70
	Wool	1.32	13-15	5	0.27~0.40
ABF fibre	Nylon	1.14	4.1-4.5	100	0.40~0.70

558

*Recommended by the manufacturer

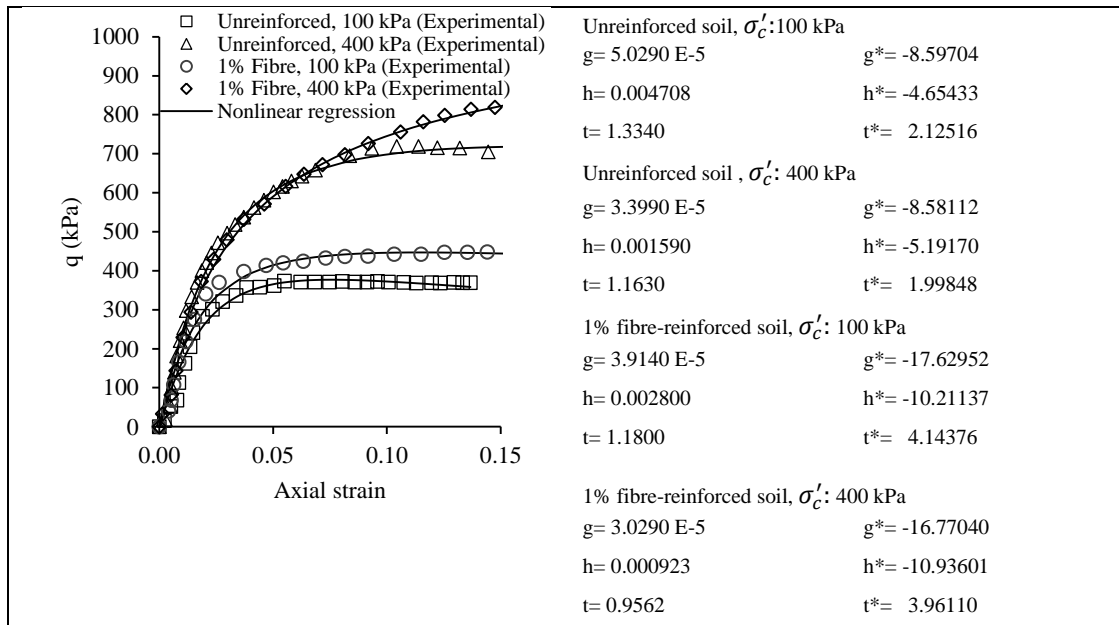
559

Table 3. Comparison of experimental and predicted shear strength results

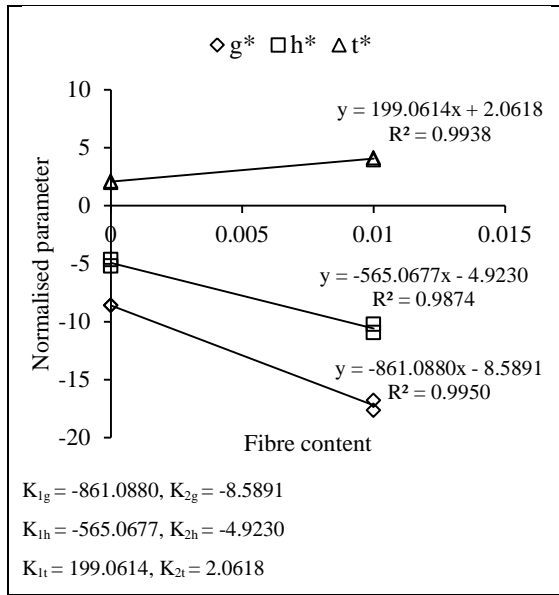
Test data	$\frac{(\frac{q}{p'})_{predicted}}{(\frac{q}{p'})_{experiment}}$	$\frac{q_{predicted}}{q_{experiment}}$	
$\varepsilon = 14.5\%, f = 0.5\%, \sigma'_c = 50 \text{ kPa}$	1.12	1.02	Babu and Chouksey (2010)
$\varepsilon = 14.3\%, f = 1\%, \sigma'_c = 50 \text{ kPa}$	1.08	0.87	
$\varepsilon = 14.3\%, f = 2\%, \sigma'_c = 50 \text{ kPa}$	1.06	0.81	
$\varepsilon = 14.4\%, f = 0.5\%, \sigma'_c = 100 \text{ kPa}$	1.03	1.16	
$\varepsilon = 14.4\%, f = 1\%, \sigma'_c = 100 \text{ kPa}$	0.99	1.12	
$\varepsilon = 14.4\%, f = 2\%, \sigma'_c = 100 \text{ kPa}$	0.94	1.08	
$\varepsilon = 14.5\%, f = 0.5\%, \sigma'_c = 150 \text{ kPa}$	0.96	1.15	
$\varepsilon = 14.5\%, f = 1\%, \sigma'_c = 150 \text{ kPa}$	0.90	1.14	
$\varepsilon = 14.4\%, f = 2\%, \sigma'_c = 150 \text{ kPa}$	0.85	1.05	
$\varepsilon = 13.6\%, f = 0.5\%, \sigma'_c = 100 \text{ kPa}$	-	1.06	Wu et al. (2014)
$\varepsilon = 14.4\%, f = 1\%, \sigma'_c = 100 \text{ kPa}$	-	0.94	
$\varepsilon = 14.4\%, f = 1.5\%, \sigma'_c = 100 \text{ kPa}$	-	0.96	
$\varepsilon = 14.1\%, f = 0.5\%, \sigma'_c = 200 \text{ kPa}$	-	0.98	
$\varepsilon = 14.1\%, f = 1\%, \sigma'_c = 200 \text{ kPa}$	-	1.03	
$\varepsilon = 14.3\%, f = 1.5\%, \sigma'_c = 200 \text{ kPa}$	-	0.93	
$\varepsilon = 14.1\%, f = 1.5\%, \sigma'_c = 300 \text{ kPa}$	-	0.98	
$\varepsilon = 14.1\%, f = 1.5\%, \sigma'_c = 400 \text{ kPa}$	-	1.01	
$\varepsilon = 14.7\%, f = 10\%, \sigma'_c = 100 \text{ kPa}$	-	1.08	Ozkul and Bykal (2007)
$\varepsilon = 13.6\%, f = 10\%, \sigma'_c = 200 \text{ kPa}$	-	1.01	
$\varepsilon = 14.2\%, f = 10\%, \sigma'_c = 300 \text{ kPa}$	-	0.99	
$\varepsilon = 10.5\%, f = 0.3\%, \sigma'_c = 600 \text{ kPa}$	-	0.94	Nguyen and Fatahi (2016)
$\varepsilon = 10.5\%, f = 0.5\%, \sigma'_c = 600 \text{ kPa}$	-	0.95	
$\varepsilon = 10.5\%, f = 0.3\%, \sigma'_c = 800 \text{ kPa}$	-	0.88	
$\varepsilon = 10.5\%, f = 0.5\%, \sigma'_c = 800 \text{ kPa}$	-	0.90	
$\varepsilon = 14.2\%, f = 0.4\%, \sigma'_c = 78.48 \text{ kPa}$	0.88	-	Khatri et al. (2016)
$\varepsilon = 14.1\%, f = 1.6\%, \sigma'_c = 78.48 \text{ kPa}$	0.97	-	
$\varepsilon = 14.1\%, f = 0.4\%, \sigma'_c = 156.96 \text{ kPa}$	1.04	-	
$\varepsilon = 14.2\%, f = 1.6\%, \sigma'_c = 156.96 \text{ kPa}$	1.06	-	
$\varepsilon = 14.1\%, f = 0.4\%, \sigma'_c = 313.92 \text{ kPa}$	1.22	-	
$\varepsilon = 14.5\%, f = 1.6\%, \sigma'_c = 313.92 \text{ kPa}$	1.12	-	

562 **SUPPLEMENTAL MATERIAL**
 563

564 In this example, the model parameters of the introduced modified hyperbolic model are calculated for experimental
 565 data reported by Wu et al. (2014). A nonlinear regression analysis using the modified hyperbolic function (Eq. 5)
 566 was carried out on the stress-strain data of the unreinforced and 1% fibre-reinforced soil tested at effective
 567 consolidation stresses of 100 kPa and 400 kPa, respectively. **Figure S1** shows the yielded modified hyperbolic and
 568 normalised modified hyperbolic regression model parameters (**Equations 9 to 11**) for calibrating the model. In order
 569 to determine the linear coefficients ($k_{1a,g}$, $k_{2a,g}$, $k_{1b,h}$, $k_{2b,h}$, $k_{1n,t}$ and $k_{2n,t}$), draw a graph of normalised modified
 570 hyperbolic model parameters versus fibre content and find the best fit line (See **Figure S2**). Then use **equations 15**
 571 to **17** to calculate the modified hyperbolic model parameters (g, h and t). Finally, use **equation 5** or **19** to predict the
 572 deviator stress of the fibre-reinforced clay.
 573



574 Figure S1. Experimental data and modified hyperbolic nonlinear regression analysis of deviator stress of
 575 unreinforced and fibre-reinforced soil (Wu et al., 2014)
 576



577 Figure S2. Relationship between normalised modified hyperbolic parameters and fibre content